

Collision Processes of Hydrocarbon Species in Hydrogen Plasmas: I. The Methane Family

R. K. Janev^{1,2} and D. Reiter^{1,3}

Abstract

Cross sections and rate coefficients are provided for collision processes of CH_y and CH_y^+ ($1 \leq y \leq 4$) hydrocarbon species with electrons and protons in a wide range of collision energy and temperature. The considered processes include: electron-impact ionisation and dissociation of CH_y , dissociative excitation, ionisation and recombination of CH_y^+ with electrons, and charge- and atom exchange in proton collisions with CH_y . In dissociative processes all important reaction channels are considered separately. Information is also provided about the energetics for each individual reaction channel. The cross sections and rate coefficients are represented in analytic fit forms.

¹Institut für Plasmaphysik, Forschungszentrum Jülich GmbH, EURATOM Association, Trilateral Euregio Cluster, D-52425 Jülich, Germany

²Macedonian Academy of Sciences and Arts, 1000 Skopje, Macedonia

³Institut für Laser- und Plasmaphysik, Heinrich-Heine-Universität, D-40225 Düsseldorf, Germany

Contents

1	Introduction	3
2	Determination of Cross Sections and Reaction Energetics	6
2.1	Electron Impact Ionisation of CH_y	6
2.2	Electron Impact Dissociation of CH_y to Neutrals	10
2.3	Electron Impact Dissociative Excitation of CH_y^+	14
2.3.1	“proper” DE processes for CH_y^+	15
2.3.2	CAD processes for CH_y^+	17
2.4	Dissociative Ionisation of CH_y^+ Ions	18
2.5	Dissociative Recombination of Electrons with CH_y^+ Ions	19
2.6	Charge Exchange and Particle Rearrangement Processes in $\text{H}^+ + \text{CH}_y$ Collisions	21
3	Analytic Representations of the Cross Sections	23
3.1	Electron Impact Ionisation of CH_y	23
3.2	Electron Impact Dissociation of CH_y to Neutrals	23
3.3	Dissociative Excitation of CH_y^+ by Electron Impact	24
3.4	Dissociative Ionisation of CH_y^+ by electron impact	25
3.5	Dissociative Recombination of Electrons with CH_y^+	25
3.6	Charge Exchange and Particle Exchange Processes	26
4	Reaction Rate Coefficients	27
5	Concluding Remarks	30
6	References	33
7	Appendix: Tables	37

1 Introduction

Because of its low atomic number (i.e. low radiative capacity) and its capability to withstand high heat fluxes, carbon (in form of graphite or carbon-carbon composites) continues to be used as plasma facing material in most presently operating fusion devices (e.g. JET, JT-60U, D-III D, LHD, ASDEX-U, TEXTOR, etc.), and it is the leading candidate for such materials in the divertor designs of next-generation fusion machines [1].

This is the case despite one of the most critical current design problems for fusion devices related to this material, namely the carbon re-deposition and tritium co-deposition problem. On JET, operated with tritium, the tritium inventory was found to build up without saturation limit.

This problem may be so serious as to rule out the use of carbon in fusion devices. That would, however, eliminate that material that, by a considerable margin, we know most about. It therefore would be a setback for fusion research driven to the extreme [2].

There are several sub-components to this problem, such as large scale convection in the SOL, the source of carbon at the walls, and the plasma chemistry and neutral hydrocarbon transport. In order to separate the first two of these from the third, by means of numerical plasma edge simulation codes, a detailed and accurate knowledge of the cross sections of the relevant plasma chemical processes is required. This will be provided by the present report for the methane family of hydrocarbons.

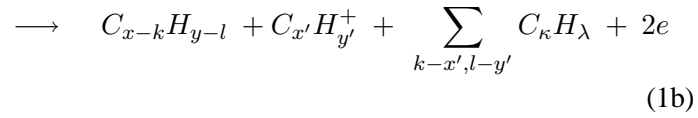
The interaction of hydrogenic plasma with the wall carbon materials leads to generation of hydrocarbon molecules C_xH_y that are released into the plasma. In subsequent collisions with plasma electrons and protons, C_xH_y molecules are ionised and dissociated, producing a broad spectrum of $C_{x'}H_{y'}$ and $C_{x'}H_{y'}^+$ ($1 \leq x' \leq x$; $1 \leq y' \leq y$) hydrocarbon species, as well as H, H_2 , C and their ions. Under divertor plasma conditions (temperatures in the range ~ 1 -20 eV), the fragmentation processes of C_xH_y and $C_xH_y^+$ species leading to the final fragmentation products C and H (and their ions) may not be extremely fast, which poses the problem of their transport in the plasma. The study of hydrocarbon (or carbon) transport in the plasma, or the use of any plasma diagnostics based on characteristic features of hydrocarbons (or carbon), e.g., radiation, requires accurate information on the cross sections (or rate coefficients) for all important collision processes and for all hydrocarbon species present in the plasma.

Laboratory experiments show that under hydrogen ion (or atom) bombardment

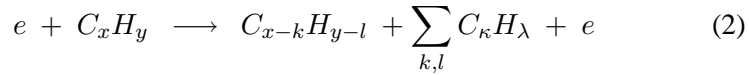
of carbon materials with impact energies typical for a divertor plasma (sub-eV to 10-20 eV), important contributions to the released hydrocarbon fluxes come from CH₃, CH₄, C₂H₂, C₂H₄, C₂H₆, C₃H₄, C₃H₆ and C₃H₈ [3,4].

The most important electron-impact processes of C_xH_y and C_xH_y⁺ molecules (molecular ions) are (the summation signs below have only a symbolic meaning, indicating the various reaction products for different channels):

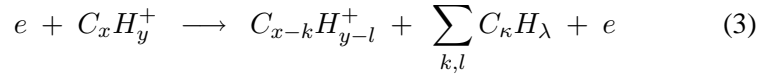
1) Direct (I) and dissociative (DI) ionisation of C_xH_y :



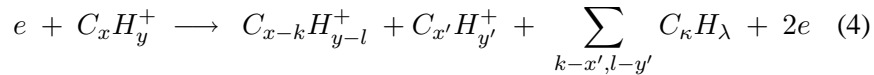
2) Dissociative excitation (DE) of C_xH_y neutrals:



3) Dissociative excitation (DE) of C_xH_y⁺ ions:



4) Dissociative ionisation (DI) of C_xH_y⁺ ions:



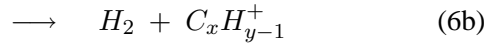
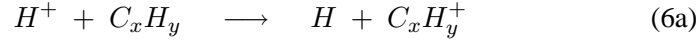
5) Dissociative recombination (DR):



where the summations in (1) - (5) go over all dissociative channels.

The processes of dissociative ionisation of C_xH_y⁺ ions (4) have much higher energy thresholds ($E_{th} \geq 25$ eV) than the dissociative excitation to neutrals ($E_{th} \sim 10$ eV) and, at least in cold divertor plasmas, their role is expected to be less important. However we include them here for completeness, and because chemical erosion at main chamber components or in limiter tokamaks can produce such ions traveling in a plasma much hotter (with T_e well above E_{th}) than typical of divertor plasmas.

The most important processes of plasma protons with C_xH_y molecules are:

6) charge exchange and particle rearrangement (CX):

of which the rearrangement channel (6b) is important only at collision energies below ~ 1 eV.

The number of reactions represented by Eqs. (1) - (6) for the C_xH_y and $C_xH_y^+$ species with $1 \leq x \leq 3$ and $1 \leq y \leq 2x+2$ is very large (more than 200 important reactions for the 36 hydrocarbon species involved). On the other hand, the experimental (or theoretical) cross section information on these reactions is very limited. It covers mainly the chemically “stable” species (non-radicals) and in most cases only the total (“gross”) cross sections (without identification of the individual reaction channels). In plasma modeling applications, however, a complete set of channel resolved cross section data is required for a given family (or families) of hydrocarbons (C_xH_y and $C_xH_y^+$ with fixed x). In this situation, the unavailable cross section information has to be generated on the basis of the available one by using certain physical arguments, most frequently certain cross section scaling rules. Such an approach has been used in the first collection of collisional hydrocarbon data for the methane family (CH_y , CH_y^+ , with $1 \leq y \leq 4$) [5], and in a more recent publication [6] covering the heavier hydrocarbons C_2H_y and C_3H_y ($1 \leq y \leq 6$). The success of this approach for “derivation” of cross section data for which no experimental (or theoretical) information is available in the literature depends on how accurate are the basic data used in the scaling procedures and how well physically based (and established) are the applied cross section scaling rules. Both these criteria were, in our opinion, not adequately met in the collections [5] and [6]. With the passage of time, the experimental cross section database for collisional processes of hydrocarbons with electrons and protons has continued to increase, and recent developments of experimental techniques (especially the use of storage rings) have started to produce very accurate (of about 10-15%) and channel resolved cross section information for many of these processes (notably for dissociative ionisation, excitation and recombination). The understanding of basic physical mechanisms governing these processes has also continued to advance in recent years, providing a better insight in the cross section scaling laws (and their ranges of validity). On this new basis, complete databases have recently been assembled for the electron-impact ionisation (direct and dissociative), [7], and proton charge exchange [8] processes of hydrocarbons C_xH_y with $1 \leq x \leq 3$ and $1 \leq y \leq 2x+2$.

The purpose of the present report is to provide a complete set of cross section data for all the processes (1) - (6) for the methane family of hydrocarbons (CH_y , $1 \leq y \leq 4$), with taking into account the most recent experimental information and understanding of their basic physics. Information about the energetics (energy gain-loss) of individual reaction channels, also required as input in kinetic (e.g. Monte-Carlo-) transport codes [9], will also be provided.

The organization of this report is as follows. In the next section we give the sources of experimental (or theoretical) data used as a basis for recommended cross sections, and explain the procedures for deriving the cross sections unavailable in the literature. The information on reaction energetics is also provided there. In section 3, we give analytic expressions for the total and reaction channel cross sections. In section 4 we give analytic expressions for the rate coefficients for some of the processes studied here. The summary and concluding remarks are given in section 5.

Graphs of the cross sections and reaction rate coefficients as well as the analytic fitting coefficients are provided for downloading on the web domain www.eirene.de of the EIRENE code, in the atomic and molecular data section.

2 Determination of Cross Sections and Reaction Energetics

2.1 Electron Impact Ionisation of CH_y

The experimental database and scaling procedures used to determine the cross sections σ_I for direct and σ_{DI} for dissociative ionisation of CH_y ($1 \leq y \leq 4$) by electron impact have been described in detail in Ref. [7]. Here we give only a brief account of them, with some emphasis on the differences with Ref. [5].

Accurate (to within 10%) total ionisation cross section measurements exist only for CH_4 , [10-12] in the energy range from threshold to 12 KeV. For CH_3 , CH_2 and CH there exist total cross section calculations performed by using the Binary-Encounter-Bethe (BEB) model [13, 14]. Very accurate partial ionisation cross section measurements have been recently performed for the direct and for the six dissociative ionisation channels of CH_4 [15, 16], the sum of which is in perfect (to within 10%) agreement with the directly measured total cross section. Except for the dominant $\text{CH}_4^+ + e$ and $\text{CH}_3^+ + \text{H} + e$ ionisation channels, the earlier partial cross section measurements of Refs. [17-19] for the $\text{CH}_2^+ + \text{H}_2 + e$, $\text{CH}^+ + \text{H}_2 + \text{H} + e$ and other (weaker) ionisation channels differ by more than 30

- 40% from those of Refs. [15,16]. We note that the data of Refs. [17-19] were used in the database of Ref. [5].

Partial cross section measurements for CH_y ($y = 2, 3$) have been performed in Ref. [20] and for CD_y ($y = 1, 2, 3$) in Ref. [21] but only for the direct ionisation channel ($\text{CH}_y \rightarrow \text{CH}_y^+ + e$) and one dissociative ionisation channel ($\text{CH}_y \rightarrow \text{CH}_{y-1}^+ + \text{H} + e$). (There is no isotope effect in the direct and dissociative ionisation channels.) Both sets of data cover the energy range from threshold to 200 eV and agree well with each other (within their experimental uncertainty of about 10 - 15%). In Ref. [5] only these two reaction channels for the CH_y ($y = 1-3$) molecules were included (based on the data of Ref. [20]), while in Ref. [7] (as well as in the present report) additional dissociative ionisation channels are included.

Table 1 gives the list of all important ionisation channels for CH_y ($y = 1-4$) molecules which are included in the present database. In the same table we give the values of ionisation (I_p) and appearance (A_p) potentials (threshold energies) for the direct and dissociative ionisation channels, respectively, obtained on the basis experimental and thermochemical data given in Ref. [22].

As mentioned above, only for the CH_4 molecule there exist experimental cross sections for all dissociative channels listed in Table 1. For the other CH_y ($y = 1-3$) molecules such information, besides for the direct ionisation, exist only for the $\text{CH}_{y-1}^+ + \text{H} + e$ dissociation channels. In order to determine the cross sections for other dissociative ionisation channels for CH_y ($y = 1-3$) molecules, use of additivity rules for the strengths of chemical bonds in polyatomic molecules has been made in Ref. [7]. These rules, discovered many years ago [23], do not lose their validity when the molecule is subjected to long-range forces or to delocalisation of its free charge (as it happens during the collisions) [24]. A manifestation of these additivity rules was the observation in Ref. [11] that total electron-impact ionisation cross sections for a large number of hydrocarbon molecules C_xH_y , with x up to $x = 5$ and y up to $y = 12$, show a remarkable linear dependence on the number x of C atoms in C_xH_y for the high collision energies (above 600 eV) at which the experiments were performed.

The analysis of more recent total ionisation cross section data for the hydrocarbon molecules has showed that x-linearity of total cross sections remains valid down to very low ($\sim 20-30$ eV) energies [7]. Moreover, the validity of additivity rules was checked also with respect to the number y of H atoms in C_xH_y molecules (with fixed x) and it was found that the y-linearity is rigorously preserved for the CH_y , C_2H_y and C_3H_y hydrocarbon families [7]. It was, further, demonstrated in

Ref. [7], that, not surprisingly, the additivity rules for the strengths of chemical bonds result also in linear y -dependencies of the partial ionisation cross sections. (For the direct ionisation cross sections of CD_y ($y = 1-4$) the y -linearity was first observed in Ref. [21] for the energy of 100 eV.)

A further consequence of the additivity rules is that the ratios of partial cross sections for different ionisation channels also have a linear dependency on y . This opens the possibility that, knowing the cross section ratios for different channels in CH_4 (which is our case) and the total cross sections of CH_4 and CH , one can determine the partial ionisation cross sections for all CH_y ($y = 1-3$) molecules. Based on the experimental estimates in Ref. [11] we know the cross section for direct ionisation and for the C^+ production channel. Furthermore a contribution of 2% to the total cross section for CH ionisation was assigned in Ref. [7] to the $C + H^+ + e$ dissociative ionisation channel for energies above ~ 30 eV, thus determining $\sigma_{I+DI}^{tot}(CH)$ for $E \geq 30$ eV. Another important consequence of the additivity rules (observed earlier in Ref. [25] for a large number of hydrocarbon molecules and further demonstrated in Ref. [7]) is that the fractional contributions of various ionisation channels to the total ionisation cross section remain energy invariant in the energy region above $\sim 30-40$ eV, i.e., sufficiently far from the energy thresholds of all important ionisation channels. This fact has also been used in Ref. [7] to determine the experimentally unknown dissociative ionisation cross sections for the CH_y ($y = 1-3$) molecules. In the energy region below 20-30 eV, the ionisation cross section is predominantly determined by its threshold behavior, which experimental information shows to be (approximately) of the form $(1 - E_{th} / E)^3$, where E_{th} is the threshold energy (I_p or A_p in Table 1).

Kinetic Monte-Carlo particle transport modeling codes require information not only about the rate coefficient of a particular reaction but also information about the momentum and energy distribution of reaction products [9]. Required also in these codes is the energy lost (or gained) by the reactants (including any involved electrons) in the reaction. The total energy and momentum of the collision system are, of course, conserved. The determination of these quantities in the case of inelastic electron collisions with CH_y (or CH_y^+) molecules (ions) requires a detailed knowledge of the potential energy surfaces of ground and excited states of these molecules and their ions. Except for the CH and CH^+ systems (see, e.g. Ref.[26-29]), such information is not available (or extremely sporadic) in the literature. In this situation, certain assumptions have to be made about the potential energies of dissociating electronic states of CH_y and CH_y^+ ($y = 2-3$) molecular

systems in order to calculate at least the mean electron energy loss and the mean total kinetic energy of dissociation products in the considered electron-impact inelastic processes. The assumptions on the energies of dissociating potential energy surfaces are made on the basis of plausible theoretical arguments and in several cases they are supported by experimental measurements of the kinetic energy of dissociated products.

For the direct ionisation channel, $\text{CH}_y \rightarrow \text{CH}_y^+ + e$, the energy lost by the electron coincides with the ionisation potential I_p . For the dissociative ionisation channels, the appearance potential A_p , as given in Table 1, corresponds to the (unexcited) products with zero kinetic energy. (Throughout this report we assume that the initial target, CH_y or CH_y^+ , is in its ground vibrational state.) Such “direct” transition of CH_y molecules to the vibrational continuum of CH_y^+ ions is, of course, possible (as indicated by the closeness of experimentally observed appearance potentials with the A_p values in Table 1 in many cases), but its cross section is not expected to be large. Much stronger is the transition from the ground state of CH_y to an excited, dissociative electronic state of CH_y^+ which produces the products $A^+ + B + e$ (sometimes $A^+ + B + C + e$, see Table 1). In order to reach the dissociative potential surface of excited ionic state $(A^+, B)_{exc}$, the incident electron should spend an amount of energy

$$E_{el}^{(-)} = I_p(\text{CH}_y) + E_{exc}(\text{AB}^+) \quad (7)$$

where $I_p(\text{CH}_y)$ is the ionisation potential of CH_y and $E_{exc}(\text{AB}^+)$ is the excitation energy of $(\text{AB}^+)_{exc}$ state of the CH_y^+ ion. Assuming that the Franck-Condon regions of the ground vibrational states of CH_y and CH_y^+ significantly overlap, the energy $E_{exc}(\text{AB}^+)$ is given by

$$E_{exc}(\text{AB}^+) = D_0^{(+)}(\text{AB}^+) + \Delta E_{exc}(\text{AB}^+) \quad (8)$$

where $D_0^{(+)}(\text{AB}^+)$ is the dissociation energy of CH_y^+ for production of $A^+ + B$ fragments (with zero kinetic energy), and $\Delta E_{exc}(\text{AB}^+)$ is the energy of excited $(\text{AB}^+)_{exc}$ state above the $A^+ + B$ dissociation limit. The energy $\Delta E_{exc}(\text{AB}^+)$ is released in the dissociation process and constitutes the total kinetic energy E_K of reaction products A^+ and B .

Since the Franck-Condon region of the ground vibrational state of CH_y has a finite range, it is obvious that both $E_{el}^{(-)}$ and $\Delta E_{exc}(\text{AB}^+) \equiv E_K$ have a certain (Gaussian type) distribution (with maximum corresponding to the transition from the center of Franck-Condon region). In Table 1, the mean values of these quanti-

ties (averaged over the Franck-Condon region of ground vibrational state of CH_y) are given.

We note that relations (7) and (8) hold irrespective whether the final products A^+ and B are internally excited or not. The total kinetic energy E_K released in the dissociative process is shared among the products inversely proportionally to their masses. If the number of dissociated products is N , with masses M_1, M_2, \dots, M_N , then the kinetic energy of the product j with M_j is given by

$$E_{K,j} = \frac{\mu}{M_j} \cdot \Delta E_{exc}(\text{AB}^+) \quad (9)$$

where μ is the reduced mass of the products.

Since the value of $D_0^{(+)}(\text{AB}^+)$ can be calculated from thermochemical tables for the heat of formation [22] for any dissociative channel of CH_y^+ ions, and since the ionisation potentials I_p of CH_y molecules are known (see e.g. again Ref. [22]), the only unknown quantity in Eqs. (7) and (8) for the CH_y^+ ions (except for CH^+) is $\Delta E_{exc}(\text{AB}^+)$. The experimental measurements of the energies of dissociation fragments in the $e + \text{CH}_4$ collision system at different impact energies [30-36] have shown that, to a good approximation, the relations

$$\Delta E_{exc}(\text{AB}^+) = k_1 D_0(\text{AB}^+), \quad \Delta E_{exc}(\text{AB}) = k_2 D_0(\text{AB}) \quad (10)$$

with $k_1, k_2 \simeq 0.8 - 2.5$, hold. The second of above relations applies for the dissociation of CH_y to neutral fragments only, with $D_0(\text{AB})$ being the dissociation limit of CH_y for the $\text{A} + \text{B}$ products. Relations (10), with the indicated values of k_1 and k_2 are confirmed also in the CH/CH^+ system for which the potential energies of lower excited states are known [26-29]. For majority of dissociation channels in the $\text{CH}_4/\text{CH}_4^+$ and CH/CH^+ systems, the values of constants k_1 and k_2 are found to be close to one. The closeness of $\Delta E_{exc}(\text{AB})$ and $D_0(\text{AB})$ (or $\Delta E_{exc}(\text{AB}^+)$ and $D_0(\text{AB}^+)$) can, to a certain degree, be related to the approximate ‘‘symmetry’’ in the energy splitting of bonding and anti-bonding molecular states (which is well pronounced at the large separations of the fragments). In assigning the values for $\Delta E_{exc}(\text{AB}^+)$ for the various dissociative ionisation channels in Table 1, we were guided by the above evidences and considerations.

2.2 Electron Impact Dissociation of CH_y to Neutrals

There are no direct cross section measurements for the electron impact dissociation of CH_y molecules to neutral products only (reactions (2)). The recent cross

section measurements for CH_3 and CH_2 radical production from CH_4 upon electron impact in Ref.[37] contain contributions not only from the dissociative excitation channels ($\text{CH}_3 + \text{H}$, and $\text{CH}_2 + \text{H}_2/2\text{H}$, respectively), but also from the dissociative ionisation channels ($\text{CH}_3 + \text{H}^+ + \text{e}$, and $\text{CH}_2 + \text{H}^+ + \text{H} + \text{e}$ plus $\text{CH}_2 + \text{H}_2^+ + \text{e}$, respectively). While for energies below ~ 30 eV the contributions of dissociative ionisation channels to the CH_3 and CH_2 production cross sections are small, at energies above 50-60 eV they may become important. For instance the cross section of the dissociative ionisation reaction $\text{e} + \text{CH}_4 \rightarrow \text{CH}_3 + \text{H}^+ + 2\text{e}$ has at $E = 100$ eV a value of about $5 \times 10^{-16} \text{cm}^2$, (see Appendix and Refs.[15,16]), whereas the measured CH_3 production cross section in Ref.[37] has at this energy about the same ($\simeq 5.2 \times 10^{-16} \text{cm}^2$) value. This indicates that the cross section for the $\text{CH}_3 + \text{H}$ channel should be of the order of magnitude 10^{-17}cm^2 , or smaller. For the CH_2 neutral production channel, the cross section reported in Ref.[37] at energies above 50 eV was beyond the detection possibilities of their apparatus, while the cross section for the $\text{CH}_2 + \text{H}_2^+ + \text{e}$ ionisation channel in the energy range 70-100 eV has values of about $4 \times 10^{-18} \text{cm}^2$ (see Refs.[15,16] and the Appendix). Although the cross section uncertainties claimed in Ref.[37] are rather large ($\simeq 100\%$), the sharp decrease of their cross sections for CH_3 and CH_2 production from the $\text{e} + \text{CH}_4$ collision appears to be unreasonable. Moreover, the cross sections for production of CF_3 , CF_2 and CF neutrals from the $\text{e} + \text{CF}_4$ collision system, measured by the same authors in Ref.[38] have an “expected” behavior (i.e. cross section maxima at 100-120 eV and a decrease at higher energies in accordance with $E^{-1} \ln(E)$ or E^{-1} Born laws).

Therefore, in determining the cross sections for electron impact dissociation of CH_y molecules to neutral products only we shall adopt the approach used in Ref.[5], supplemented by the use of earlier discussed additivity rules.

The total cross section for dissociation to neutrals can obviously be represented as difference of the total cross section σ_D^{tot} for dissociation of the molecule (to neutral and charged products) and the total cross section for dissociative ionisation (including multiple ionisation and production of more than one ion product)

$$\sigma_{DE}^{\text{tot}} = \sigma_D^{\text{tot}} - \sigma_{DI}^{\text{tot}}. \quad (11)$$

The cross section σ_D^{tot} for CH_4 has been measured in Ref.[39] in the energy range from threshold to 500 eV. For other CH_y ($y = 1-3$) molecules such cross section measurements presently do not exist. However, measurements of σ_D^{tot} have been performed for CF_4 , CF_3H , C_2F_6 , C_2D_6 and C_3F_8 [40] (in the energy range from threshold to 600 eV), showing that the additivity rules for the strengths of chemical

bonds are valid also for the total dissociative cross sections. On this basis one can expect that the σ_D^{tot} cross sections for CH_y ($y = 1-4$) should have a linear dependence on y .

The channel resolved experiments on direct and dissociative ionisation of CH_y ($y = 2-4$) molecules [15-21] have shown that the ion production channels with doubly charged products (or with more than one charged products) have a minor (below $\sim 5\%$) contribution to the total dissociative ionisation cross section. This is related to the much higher appearance potentials (above $\sim 30 - 40$ eV) for these channels. Therefore, in using Eq. (10) for determining the total cross section for dissociation to neutrals, σ_{DE}^{tot} , one can neglect the contribution of the multiple charged product channels to σ_{DI}^{tot} . The determination of σ_{DE}^{tot} for CH_4 up to $E = 500$ eV has been done on the basis of $\sigma_D^{tot}(\text{CH}_4)$ data from Ref.[39] and σ_{DI}^{tot} data from Refs.[15,16] (or the present report; see Appendix). For $E > 500$ eV, the cross section can be extrapolated in accordance with its Bethe-Born behavior. It should be noted that the cross section $\sigma_{DE}^{tot}(\text{CH}_4)$ determined in this way is consistent with the sum of measured CH_3 and CH_2 production cross sections of Ref.[37] in the energy range below 30 eV (within the claimed experimental uncertainties). It should also be noted that the broad maximum of σ_{DE}^{tot} appears in the same region ($\sim 70 - 90$ eV) as for $\sigma_{I+DI}^{tot}(\text{CH}_4)$. From the proportionality of $\sigma_{DE}^{tot}(\text{CH}_y)$ with $\sigma_{I+DI}^{tot}(\text{CH}_y)$ (following from the additivity rules), and knowing the ratio $\sigma_{DE}^{tot}(\text{CH}_4)/\sigma_{I+DI}^{tot}(\text{CH}_4)$, one can determine the cross sections $\sigma_{DE}^{tot}(\text{CH}_y)$ for CH_y molecules with $y = 1 - 3$, at least in the energy region above 20 - 30 eV. In the region below ~ 20 eV, the cross section is governed by its threshold behavior, $(1-E_{th}/E)^\alpha$, $\alpha \simeq 3$.

For determining the cross sections for different neutral dissociation channels of the CH_y molecule, one has to consider the operating dissociation mechanism. At least at energies above $\sim 30-40$ eV, when all dissociation channels are open, the dissociation of a CH_y molecule to neutrals only and its dissociative ionisation (dissociation to neutral and charged products) are inter-related processes. This is due to the fact that the neutral dissociation channels correspond to excited anti-bonding states of the CH_y molecule which are mixed with the repulsive states of its ion, CH_y^+ . Most of the excited states (with exception of a few, lower ones) even in the simplest CH hydrocarbon molecule are repulsive, and their potential energy curves enter the continuum of CH^+ ion at internuclear distances below $\sim 3a_0$ (where a_0 is the Bohr radius) [26-29]. Thus, most of the excitations of neutral CH_y molecular states lead to auto-ionisation (i.e. to dissociative ionisation). This picture [41] is

supported also by the numerous experimental studies of the dissociated products (their energy distribution, relative abundance, radiation properties, etc.). The picture of competing dissociative auto-ionisation and neutral dissociation processes is also supported by the observed isotope effect in the neutral dissociation channels of CH_4/CD_4 systems [42]. While the auto-ionisation is a mass independent process (governed only by the interaction of a discrete electronic state embedded into a continuum with the continuum states), the dissociation depends on time the system spends in the dissociating state embedded in the continuum, and, thus, on the masses of products.

Because of the above described common mechanism for dissociation to neutrals and dissociative (auto-)ionisation, one can expect that the contribution $R_{DE}(A)$ of a particular channel $\text{CH}_y \rightarrow A + \dots$ to the total dissociation cross section of CH_y to neutrals, will be the same as the contribution $R_{DI}(A^+)$ of dissociative ionisation channel $\text{CH}_y \rightarrow A^+ + \dots + e$ to the total dissociative ionisation cross section of CH_y , i.e.,

$$\frac{\sigma_{DE}(A)}{\sigma_{DE}^{tot}(\text{CH}_y)} = R_{DE}(A) = R_{DI}(A^+) = \frac{\sigma_{DI}(A^+)}{\sigma_{DI}^{tot}(\text{CH}_y)} \quad (12)$$

By knowing the values of $R_{DI}(A^+)$ for all dissociative ionisation channels of CH_y , and $\sigma_{DE}^{tot}(\text{CH}_y)$, one can determine $\sigma_{DE}(A)$ from Eq. (12). In the energy region above ~ 30 eV, the values of $R_{DI}(A^+)$ appeared to be only very weakly dependent on the energy. Therefore, their values at $E = 80$ eV have been ascribed to $R_{DE}(A)$. These values are given in Table 2 for all the dissociation channels of CH_y molecules. It should be mentioned that the dissociative ionisation channels $\text{CH}_4 \rightarrow \text{CH}_3^+ + \text{H} + e$ and $\text{CH}_4 \rightarrow \text{CH}_3 + \text{H}^+ + e$ are related to the neutral dissociation channels $\text{CH}_4 \rightarrow \text{CH}_3 + \text{H}$ and $\text{CH}_4 \rightarrow \text{CH}_3 + \text{H}^*$, where H^* is an excited H-atom. Since we do not distinguish the products by their state of excitation, the $R_{DE}(\text{CH}_3/\text{CH}_4)$ value in Table 2 is sum of $R_{DI}(\text{CH}_3^+/\text{CH}_4)$ and $R_{DI}(\text{H}^+/\text{CH}_4)$. (The contribution of $R_{DI}(\text{H}^+)$ to $R_{DE}(\text{CH}_3)$ is, however, less than 10%.) The R_{DE} values for neutral dissociation channels $\text{CH}_3 \rightarrow \text{CH}_2 + \text{H}$ (associated with the $\text{CH}_3 \rightarrow \text{CH}_2^+ + \text{H} + e$ dissociative ionisation channel), and $\text{CH}_3 \rightarrow \text{CH}_2 + \text{H}^*$ (associated with the $\text{CH}_3 \rightarrow \text{CH}_2 + \text{H}^+ + e$ channel) where similarly combined into the $R_{DE}(\text{CH}_2/\text{CH}_3)$ value given in Table 2.

In Table 2 are also given the threshold energies, E_{th} , mean energy loss $\overline{E_{el}^{(-)}}$ of incident electron (equal to the threshold energy) and the mean kinetic energy, $\overline{E_K}$, of the dissociation products. These quantities have been estimated on the basis of known dissociation energies of CH_y molecules for zero-kinetic energy

of dissociated products $D_0(AB)$ (“dissociation limits”) (calculated from thermochemical data in Ref.[22]), and taking that the dissociating (repulsive) state lies above the dissociation limit in the Franck-Condon region of CH_y ground state for a value $\Delta E_{exc}(AB)$ close to the dissociation limit energy $D_0(AB)$ (i.e. $k_2 \approx 1$ in Eq.(10)). The justification of this approach was discussed in the preceding subsection. The mean total kinetic energy of dissociated products is distributed among them according to Eq.(9).

2.3 Electron Impact Dissociative Excitation of CH_y^+

Total cross section measurements for the dissociative excitation (DE) of CH_y^+ ions have not been performed as yet. Cross section measurements of the $C + H^+$ dissociation channel of CH^+ ion, and of the $\text{CH} + H^+$ channel from CH_2^+ electron impact dissociation, have been performed recently in storage-ring experiments in Refs.[43] and [44], respectively. Crossed-beam measurements of the cross sections for production of H^+ and H_2^+ ions from electron collisions with all CH_y^+ ions (including CH_5^+) have also been performed [45, 46]. Since no resolution of the H^+ (or H_2^+) production channels was made in crossed beam experiments, the reported data are the sum of (at least) the dissociative excitation and dissociative ionisation cross sections of CH_y^+ ions. The contribution of dissociative ionisation processes (e.g. $C^+ + H^+ + e$ in the case of CH^+ dissociation) to the total H^+ and H_2^+ production cross sections is, however, negligible for energies below 25 - 30 eV, because of their high energy thresholds ($\sim 25 - 30$ eV). Thus, the storage-ring and crossed-beam data for C and H^+ production, respectively, from CH^+ agree perfectly well for energies below 30 eV, while those for the CH_2^+ system agree well for energies below 50 eV. From the structure of H^+ production cross sections of Refs.[45, 46] and calculated thresholds of dissociative ionisation channels for CH_y^+ ions (using the thermochemical data of Ref.[22]), one can estimate the contribution of these channels to the measured H^+ production cross sections (see next sub-section) and obtain the dissociative excitation cross sections for the channels $\text{CH}_y^+ \rightarrow \text{CH}_{y-1} + \text{H}^+$, up to the energies of 70-80 eV. The DE cross sections obtained in this way have their maxima at about 35-45 eV (except for CH^+ when the DE cross section maximum is at 25-35 eV).

The extrapolation of these derived DE cross sections in the energy region above 70-80 eV can be done in accordance with the Born-Bethe cross section behavior at high energies. It should be noted that the values of the $\sigma_{DE}(\text{H}^+)$ cross section for $\text{H}^+ + \text{neutrals}$ production from CH_y^+ ($y = 1-5$) at the energies $\sim 40-50$

eV show a strict linearity with respect to y (decreasing from $1.87 \times 10^{-16} \text{cm}^2$ for CH^+ to $0.83 \times 10^{-16} \text{cm}^2$ for CH_5^+). The measured $\sigma_{DE}(H_2^+)$ cross section values at $E \sim 30\text{-}50$ eV for CH_y^+ ($y = 3\text{-}5$) also show a similar linearity, but $\sigma_{DE}(H_2^+)$ increase with increasing y (from $0.12 \times 10^{-16} \text{cm}^2$ for CH_3^+ to $0.34 \times 10^{-16} \text{cm}^2$ for CH_5^+ at $E \sim 30\text{-}50$ eV). These linear dependencies of $\sigma_{DE}(H^+)$ and $\sigma_{DE}(H_2^+)$ on y are a manifestation of earlier mentioned additivity rules, and are expected to manifest themselves also in the cross sections of other dissociative excitation channels of CH_y^+ .

From the known dissociative excitation pattern of CH^+ ion (to $\text{C}^+ + \text{H}$ and $\text{C} + \text{H}^+$ fragments), and the experimentally known $\sigma_{DE}(H^+/\text{CH}^+)$ cross section, one can derive the total $\sigma_{DE}^{tot}(\text{CH}^+)$ cross section for the CH^+ ion by assigning a value for the $\sigma_{DE}(\text{C}^+/\text{CH}^+)$ cross section of the $\text{C}^+ + \text{H}$ fragmentation channel. The experiments [43, 45] show that the threshold energy of the $\text{CH}^+ \rightarrow \text{C} + \text{H}^+$ channel is about 4.5 - 5.0 eV, while from the known dissociative potential energy curves of CH^+ [27-29] it follows that the energy threshold of $\text{C}^+ + \text{H}$ dissociation channel is about 12.2 eV. On the basis of the large difference of threshold energies of $\text{C}^+ + \text{H}$ and $\text{C} + \text{H}^+$ channels (and the observed effects of such differences on the cross sections of other inelastic $\text{e} + \text{CH}_y$ processes; e.g., in dissociative ionisation), we have assigned a contribution of $\sigma_{DE}(\text{C}^+)$ cross section to the total dissociative excitation cross section $\sigma_{DE}^{tot}(\text{CH}^+)$ of CH^+ ion of about 10%. This gives a value of $0.18 \times 10^{-16} \text{cm}^2$ for $\sigma_{DE}(\text{C}^+)$ at energies 30 - 40 eV, where the maximum of $\sigma_{DE}^{tot}(\text{CH}^+)$ is expected (on the basis of the values of $\sigma_{DE}(H^+)$).

We should note, however, that in the case of CH^+ ions there is another process, namely electron capture to a doubly excited dissociative state of CH , which, after auto-dissociation, produces the same reaction products $\text{C}^+ + \text{H}$ as the direct DE process. This capture-auto ionisation dissociative (CAD) channel will be considered at the end of this subsection. $\sigma_{CAD}(\text{C}^+)$ is significantly larger than $\sigma_{DE}(\text{C}^+)$ [47].

2.3.1 “proper” DE processes for CH_y^+

The above mentioned approach for determining the total dissociative excitation cross sections cannot be applied for the other CH_y^+ ions because of the large number of channels involved. However, in accordance with the additivity rules, we expect that the total DE cross sections $\sigma_{DE}^{tot}(\text{CH}_y^+)$ increase with increasing y (at least in the energy range above $\sim 20 - 30$ eV). Using the similarity of dynami-

cal mechanisms governing the electron impact dissociation processes in CH_y and CH_y^+ molecular systems, we adopt that the linear increase of $\sigma_{DE}^{tot}(\text{CH}_y^+)$ with y is the same as that of $\sigma_{DE}^{tot}(\text{CH}_y)$ in the energy range above $\sim 20 - 30$ eV. (As emphasized earlier, below $E \sim 20$ eV all inelastic cross sections of CH_y and CH_y^+ are determined essentially by their threshold behavior.) For the energy of ~ 40 eV (where the maxima of $\sigma_{DE}^{tot}(\text{CH}_y^+)$ ($y = 2 - 4$) are expected), the values of $\sigma_{DE}^{tot}(\text{CH}_y^+)$ for CH_2^+ , CH_3^+ and CH_4^+ are $2.33 \times 10^{-16} \text{cm}^2$, $2.52 \times 10^{-16} \text{cm}^2$ and $2.75 \times 10^{-16} \text{cm}^2$, respectively. The value of $\sigma_{DE}^{tot}(\text{CH}^+)$ at this energy, as determined earlier, is $2.05 \times 10^{-16} \text{cm}^2$. This has been used in fixing the position of the line $\sigma_{DE}^{tot}(\text{CH}_y^+) = f(y)$ having the same slope as $\sigma_{DE}^{tot}(\text{CH}_y)$.

Knowing the total $\sigma_{DE}^{tot}(\text{CH}_y^+)$ cross sections at $\sim 30 - 40$ eV, and the $\sigma_{DE}(\text{H}^+)$ and $\sigma_{DE}(\text{H}_2^+)$ channel cross sections for all CH_y^+ , one can determine the contributions of other dissociative excitation channels to $\sigma_{DE}^{tot}(\text{CH}_y^+)$ at this energy by using their linear dependencies on y . Firstly, for the CH^+ ion we already know $\sigma_{DE}(\text{C}^+)$ at $\sim 30 - 40$ eV ($\simeq 0.18 \times 10^{-16} \text{cm}^2$). It is plausible to assume that the contribution of C^+ + neutrals channel in the case of CH_4^+ dissociation is smaller than in the case of CH^+ ion because the number of dissociative excitation channels in CH_4^+ is much larger (see Table 3). Taking this into account, as well as some other arguments connected with the weighted role of the threshold effects on the total cross section, we assign to the $\sigma_{DE}(\text{C}^+)$ cross section for the $\text{CH}_4^+ \rightarrow \text{C}^+ + \text{neutrals}$ dissociation a value of $0.12 \times 10^{-16} \text{cm}^2$. The values of $\sigma_{DE}(\text{C}^+)$ for CH_2^+ and CH_3^+ at $E \sim 40$ eV are now obtained by linear interpolation (by virtue of linearity of $\sigma_{DE}(\text{C}^+)$ from CH_y^+ as function of y). For the CH_2^+ ion, the cross sections for all dissociative excitation channels are now uniquely determined, because the value of $\sigma_{DE}(\text{CH}^+)$ is the difference between $\sigma_{DE}^{tot}(\text{CH}_2^+)$ and the cross sections for the H^+ , H_2^+ , C^+ + neutrals channels. (The $\sigma_{DE}(\text{H}^+)$ and $\sigma_{DE}(\text{C}^+)$ cross sections for CH_2^+ are each further shared between the respective $\text{H}^+ + \text{CH}$ and $\text{H}^+ + \text{C} + \text{H}$, and $\text{C}^+ + \text{H}_2$ and $\text{C}^+ + 2\text{H}$ channels, in accordance with the threshold energy weights.) A similar procedure was used for determining the channel cross sections of CH_3^+ and CH_4^+ ions (including the use of linearity of $\sigma_{DE}(\text{CH}^+)$ from CH_y^+ with y). The ratios of channel cross sections $\sigma_{DE}(A^+)$, for a particular “ A^+ + neutrals” dissociative excitation of CH_y^+ , to the total cross sections $\sigma_{DE}^{tot}(\text{CH}_y^+)$,

$$R_{DE}^+ = \frac{\sigma_{DE}(A^+)}{\sigma_{DE}^{tot}(\text{CH}_y^+)} \quad (13)$$

for the energies $E \sim 35 - 40$ eV are given in Table 3. In analogy with the case of dissociative ionisation, we expect that these ratios are weakly dependent on the

collision energy above $E \sim 20\text{-}30$ eV. (For $E \leq 20$ eV, the cross section behavior is dominated by the threshold effects.)

The values of threshold energy, E_{th} , mean electron energy loss, $\overline{E_{el}^{(-)}}$, and mean total kinetic energy of the products, $\overline{E_K}$, are also given in Table 3 for the considered dissociative excitation channels. These were determined in the same way as for other dissociative reactions in $e + CH_y$ collisions, as described in the previous two subsections.

2.3.2 CAD processes for CH_y^+

As mentioned earlier, besides by the direct DE mechanism (excitation of a repulsive state of CH_y^+ ion from its ground electronic state), the dissociation of CH_y^+ ions may be induced by electron capture into a doubly excited dissociative Rydberg state CH_y^{**} which, after auto ionisation, (ejection of the captured electron), can produce the same reaction products as the direct DE process. This capture-auto ionisation dissociation (CAD) process should have much smaller thresholds than the corresponding DE process producing the same reaction products.

There is only one cross section measurement for this process, namely the cross section for the reactions $e + CH^+ \rightarrow (CH)^{**} \rightarrow e + C^+ + H$ [47], that indicates a threshold of ~ 2.5 eV. The cross section $\sigma_{CAD}(C^+/CH^+)$ for this reaction constitutes about 70% for the cross section $\sigma_{DE}(H^+/CH^+)$ for the $CH^+ \rightarrow H^+ + C$ dissociation channel in the energy range above ~ 20 eV. The estimated total kinetic energy of the C^+ and H products from this process is about 4.0 eV.

In absence of any experimental information, or potential energy calculations of dissociative auto-ionising states, it is not possible to make a more accurate judgment about the CAD cross sections of CH_y^+ ions with $y = 2 - 4$. However, if the magnitude of the resonant structures in the dissociative recombination cross sections of CH_y^+ ions (see sub-section 2.5) is taken as a measure of the relative role of processes proceeding via the doubly excited dissociative $(CH)^{**}$ states, then, with increasing y in CH_y^+ the CAD cross section should rapidly decrease (approximately by a factor of two for each decrease of y by one). This can be also inferred from the rapid decrease of the electron capture cross section to the doubly excited state of CH_y with increasing “vertical” transition energy from the bottom of ground electronic state of CH_y^+ to the dissociative potential curve of CH_y^{**} (which increases when y increases).

2.4 Dissociative Ionisation of CH_y^+ Ions

As we have mentioned at the beginning of the preceding sub-section, the dissociative ionisation (DI) cross section for the CH^+ ion can be determined by subtracting the known $\sigma_{DE}(H^+)$ cross section [43] (up to $E \simeq 60$ eV) from the known cross section for H^+ production, $\sigma_{DE}(H^+) + \sigma_{DI}(H^+)$ [45]. For the $\sigma_{DI}(H^+)$ cross section of CH^+ ions there are also theoretical calculations [48], which agree with $\sigma_{DI}(H^+)$ derived from the experimental data, and extend the cross section into the KeV energy region. Since for CH^+ ions the only DI channel is $CH^+ \rightarrow C^+ + H^+ + e$, obviously $\sigma_{DI}(H^+) \equiv \sigma_{DI}^{tot}(CH^+)$. This cross section has its maximum at $E \simeq 80 - 100$ eV.

The main reaction channels of dissociative ionisation of CH_y^+ ions are given in Table 4. All of them are H^+ - ion production channels. Therefore, the total DI cross section for a given CH_y^+ ion is $\sigma_{DI}^{tot}(CH_y^+) \simeq \sigma_{DI}(H^+/CH_y^+)$, and can be determined from the total experimental H^+ - ion production cross section [45,46] by subtracting from it the partial $\sigma_{DE}(H^+/CH_y^+)$ cross section (determined as described in the preceding sub-section). Since the experimental H^+ -ion production cross sections are known up to the collision energy of 70 eV, the extension of $\sigma_{DI}(H^+/CH_y^+)$ to higher energies can be accomplished by using the energy invariance of the ratio $\sigma_{DI}(H^+/CH_y^+)/\sigma_{DI}(H^+/CH^+)$ in the region above ~ 50 eV. Note that $\sigma_{DI}^{tot}(CH_y^+) \approx \sigma_{DI}(H^+/CH^+)$ follows from the fact that H_2^+ -ion production cross sections measured in Ref.[46] are an order of magnitude smaller than the H^+ ion production cross sections. Besides, the threshold of H_2^+ producing DI channels are usually larger than those for the H^+ producing DI channels.

The threshold energies in Table 4 for DI channels were determined in the following way: For the CH^+ ion, for which potential energies are known [26-28], the ‘‘vertical’’ energy to reach the $C^+ + H^+$ potential energy curve from the energy minimum of CH^+ ground electronic state is $\simeq 29.0$ eV. It lies 11.78 eV above the $(C^+ + H^+)$ dissociation limit (infinite internuclear distances). The amount of 11.78 eV is the Coulomb interaction energy of C^+ and H^+ ions, after the Franck-Condon transition from the CH^+ ground electronic state to the $(C^+ + H^+)$ dissociating state is accomplished. This (interaction) energy depends on the ion charges only and has been added to the calculated dissociation energies (using thermochemical tables, Ref.[22]) of all DI channels in Table 4. The charged reaction products share the amount of 11.78 eV according to Eq.(9). The neutral products in DI channels of Table 4 have zero kinetic energy.

The ratios of channel cross sections $\sigma_{DI}(A^+/CH_y^+)$ for a given DI reaction

channels producing $A^+ + H^+$ to the total cross sections $\sigma_{DI}^{tot}(CH_y^+)$,

$$R_{DI}^+(A^+/CH_y^+) = \frac{\sigma_{DI}(A^+/CH_y^+)}{\sigma_{DI}^{tot}(CH_y^+)} \quad (14)$$

are also given in Table 4. These ratios have been calculated by using the observed $E_{th}^{-1.55}$ dependence of $\sigma_{DI}^{tot}(CH_y^+)$ in the threshold region and assuming that any two $R_{DI}^+(A_1^+/CH_y^+)$ and $R_{DI}^+(A_2^+/CH_y^+)$ branching ratios have the same energy dependence (if any) in the threshold region. Then ,

$$R_{DI}^+(A_1^+/CH_y^+)/R_{DI}^+(A_2^+/CH_y^+) \approx \left(\frac{E_{th,2}}{E_{th,1}} \right)^{1.55},$$

where $E_{th,1}$ and $E_{th,2}$ are the threshold energies for the $A_1^+ + H^+$ and $A_2^+ + H^+$ DI channels. Using these ratios and the conditions that $R_{DI}^+(A_i^+/CH_y^+)$ should sum up to one, we obtained the R_{DI}^+ values given in Table 4. Under the assumption made in their derivation they should be valid at all energies.

2.5 Dissociative Recombination of Electrons with CH_y^+ Ions

Systematic measurements of total dissociative recombination cross sections of electrons with CH_y^+ ions ($y = 1-5$) have been performed in Ref.[49] by the merged-beam method, in the energy range 0.02 - 1.7 eV. It has been recognized later, however, that due to a calibration error, the reported cross sections in Ref.[49] are by a factor of two too large [50]. These, uncorrected, cross sections were used in the compilation [5]. More recently, accurate ($\sim 10\%$) total cross section measurements were carried out by using storage rings, for CH^+ [51], CH_2^+ [44], CH_3^+ [52] and CH_5^+ [53], and in a much broader energy range (from $10^{-2} - 10^{-3}$ to 10 - 20 eV). Moreover, the use of storage rings made it also possible to determine experimentally the branching ratios of the various dissociation channels in $e + CH_y^+$ recombination. It turned out that, contrary to certain theoretical assertions [54, 55], the three-body fragmentation becomes increasingly more important than the two-body dissociation with the increase of complexity of the ion. In the present database, the total recombination cross section and the dissociation branching ratios from these recent experimental sources have been used, except for the CH_4^+ for which the total cross section data of Ref.[49] (reduced by a factor of two) have been taken. The dissociation branching ratios for CH_4^+ have been determined by interpolation between the values of corresponding dissociation channels for CH_3^+ and CH_5^+ .

The dissociative recombination channels for $e + \text{CH}_y^+$ ($y = 1-4$) collision systems are shown in Table 5, together with the values of branching ratios R_{DR} of individual channels. It should be mentioned that these branching ratios were determined at collision energies below ~ 0.1 eV (e.g. for CH_2^+), where they do not vary with the energy. However, as the dissociation H_3^+ ion indicates [56], this may change at higher energies. In Table 5 we also give the total kinetic energy of the dissociated products, $E_K^{(0)}$, calculated (using Ref.[22]) under the assumption that both CH_y^+ ion and the products are in their ground states, and for the case when the recombining electron has zero energy. For an electron with a finite energy, its center-of-mass system energy should be added to the values of $E_K^{(0)}$ given in Table 5.

It should be, however, noted that the dissociative recombination process, by its physical nature (electron capture to a doubly excited state of CH_y molecule), generally produces excited products. The question of quantum states of dissociative recombination products has been experimentally investigated only for the case of $e + \text{CH}^+$ recombination [51]. This study indicates that even at “zero” impact electron energy, predominantly populated are the first two excited states of C, i.e. the channels $\text{C}(^1\text{D}) + \text{H}(1s)$ and $\text{C}(^1\text{S}) + \text{H}(1s)$, with branching ratios 0.79 and 0.21, respectively. These channels remain dominant up to $E_{CM} \simeq 0.3$ eV, but with different branching ratios (0.75 and 0.25, respectively, see Table 5). With further increase of electron impact energy, the higher excited states of C become dominantly populated, and for $E_{CM} \geq 9$ eV, the $\text{H}(nl)$ states begin to be populated. The fulfillment of conditions for favorable population of new excited product recombination channels when collision energy increases, produces resonance structures in total recombination cross sections. These structures have been seen in the total recombination cross sections for all CH_y^+ ions, and they are particularly pronounced in the energy region above ~ 1 eV (with strong peaks at $\sim 1 - 2$ eV and $\sim 9 - 10$ eV).

From the detailed study of excited product states in $e + \text{CH}^+$ recombination [51] and the fact that the main high-energy resonance peaks in all $e + \text{CH}_y^+$ ($y = 1-5$) systems appear approximately at same energies ($\sim 1 - 2$ eV and $\sim 9 - 10$ eV), one can infer that for energies below $\sim 8-9$ eV the hydrogenic recombination products H and H_2 are electronically still not excited. One can, therefore, expect that the C atoms in the $\text{C} + \text{H}_2$ and $\text{C} + \text{H} + \text{H}$ channels of $e + \text{CH}_2^+$ recombination will have a similar quantum state distribution as in the case of $e + \text{CH}^+$ recombination for energies below $\sim 8 - 9$ eV (see Table 5). The CH molecule in the $\text{CH} + \text{H}$

dissociative channel of $e + CH_2^+$ recombination should be both electronically and vibrationally excited. Taking into account these considerations, the values of $E_K^{(0)}$, given in Table 5 for the unexcited products, have to be reduced by the amount of excitation energy of the products.

Another important result of the detailed study of reaction products in $e + CH^+$ recombination [51] is that the angular distribution of dissociated products (in the C.M. system) is not isotropic. The angular distribution anisotropy of products is different for different excited product channels and varies with energy. It becomes isotropic only in the limit of zero energy of recombined electrons. However, in a plasma with temperatures higher than ~ 0.5 eV, the CH^+ (as well as other CH_y^+) ions are rotationally (perhaps even highly) excited, so that averaging over the rotation of internuclear axis (with respect to the electron velocity vector) results in an isotropic distribution of dissociation products.

2.6 Charge Exchange and Particle Rearrangement Processes in $H^+ + CH_y$ Collisions

The cross section data for charge and particle exchange processes (6a) and (6b) have been discussed in detail in Ref.[8] for all C_xH_y ($x = 1 - 3, 1 \leq y \leq 2x + 2$) molecules. Here we give a brief account of the data for the CH_y ($1 \leq y \leq 4$) molecules only.

Total charge exchange cross section measurements for $H^+ + CH_y$ ($y = 1 - 4$) collision systems are available only for the CH_4 molecule [57-63], and cover the collision energy range from ~ 200 eV/AMU to several MeV/AMU. More recently [64], charge exchange cross sections measurements were performed for the $O^+ - CH_4$ collision system down to collision energies of about 10 eV/AMU, which due to (practically) the same ionisation potentials of O and H, can be considered as an extension of proton impact data. (The data for O^+ and H^+ projectiles are indeed the same in the overlapping energy region, and those for O^+ at energies below 200 eV/AMU conserve the trend of behaviour of $H^+ + CH_4$ cross section data.) In the energy region below ~ 10 KeV/AMU, the $H^+ + CH_4$ charge exchange cross section shows a behavior typical for resonant charge exchange processes (a logarithmic increase of the cross section with the decrease of energy, [65]). Although the $H^+ + CH_4$ charge exchange reaction is exothermic by ~ 1.1 eV, the resonant conditions for the electron capture process are nevertheless fulfilled because the reaction exothermicity can be easily expended on excitation of internal degrees of freedom of CH_4^+ reaction product. A similar resonant behavior of the cross section

is expected also for the $H^+ + CH_3$ charge exchange reaction. However, for CH_2 and CH molecules the number of internal degrees of freedom (different modes of vibrational motion, rotations within a given vibrational mode) are reduced, and the fulfillment of resonant conditions for the process becomes more difficult. Therefore, for CH_2 and CH , the cross sections as function of the collision energy should behave as those typical for non-resonant charge exchange processes (with a broad maximum in the range 1 - 20 KeV/AMU and decrease with decreasing the energy, [65]). Using the parameters for $H^+ + CH$ and $H^+ + CH_2$ charge exchange reaction, and certain criteria for the position and magnitude of cross section maximum, as well as for the steepness of the slope of its decrease with decreasing the energy, the cross sections for these two reactions were derived in Ref.[8]. A further element in deriving the cross sections for these two reactions, as well as for those of CH_3 and CH_4 in the region below $\sim 1-5$ eV was the use of known total reaction rate coefficients for all these reactions in the thermal energy region [66]. These reaction rate coefficients include contributions from both the pure charge transfer (or electron capture) reaction, $H^+ + CH_y \rightarrow H + CH_y^+$, and from the particle rearrangement channel, $H^+ + CH_y \rightarrow H_2 + CH_{y-1}^+$. The total reaction rate coefficients in the thermal energy region for $H^+ + CH_y$ charge exchange and particle rearrangement reactions are given in Table 6, together with the branching ratios R_{CX} of the reaction channels. It should be noted that the rearrangement channel for the $H^+ + CH_3$ collision system is endothermic and, therefore, not included in Table 6. In this table we also give the energy defect ΔE for each reaction channel which, if not absorbed by the internal degrees of freedom of the products, would give the total kinetic energy of the products. As argued above, for the pure electron capture reactions of CH_4 and CH_3 with H^+ , the exothermicities ΔE are fully absorbed by the ro-vibrational motion of the products CH_4^+ and CH_3^+ , respectively, and the reaction products should have zero (or close to it) value of kinetic energy. In determining the values of branching ratios for charge exchange channels in $H^+ + CH_y$ thermal collisions we have taken into account that the probability of particle rearrangement channel increases with increasing of reaction exothermicity.

In Table 6, we have added also the exothermic charge exchange reaction $H^+ + C \rightarrow H + C^+$, for completeness. (This reaction is also needed in the hydrocarbon/carbon transport modeling.)

3 Analytic Representations of the Cross Sections

The cross sections determined by the procedures described in the preceding sections can all be fitted to appropriate analytic expressions to facilitate their use in hydrocarbon transport modeling codes or in other applications. The adopted analytic representations of determined cross section do not reduce the accuracy of the cross section data.

3.1 Electron Impact Ionisation of CH_y

The direct, dissociative and total electron impact ionisation cross section determined in Ref.[7] were represented by an analytic fit function of the form

$$\sigma = \frac{10^{-13}}{E \cdot I_c} \left[A_1 \ln \left(\frac{E}{I_c} \right) + \sum_{j=2}^N A_j \left(1 - \frac{I_c}{E} \right)^{(j-1)} \right] \quad (cm^2) \quad (15)$$

where I_c has a value close (or equal) to the appearance potential (expressed in eV), E is the collision energy (expressed in eV) and A_j ($j = 1, \dots, N$) are fitting parameters. The number of fitting parameters was determined from the condition that the r.m.s. of the fit is not larger than 2-3%. The number of fitting parameters N for all ionisation channel cross sections was $N = 6$, except for the total ionisation of CH for which $N=8$.

For the total and partial ionisation cross sections of the $e + \text{CH}_y$ ($y = 1-4$) collision systems, the values of I_C and A_j are given in Table 7.

For completeness, we have fitted also the electron-impact ionisation cross section of ground state C atom (taken from Ref.[67]) by the analytic expression (15), and the corresponding I_C and A_j values for this reaction are also given in Table 7.

3.2 Electron Impact Dissociation of CH_y to Neutrals

The total electron impact dissociation cross sections of CH_y to neutral fragments (dissociative excitation), determined in sub-section 2.2., can be represented by the following simple analytic expression ($y = 1-4$)

$$\sigma_{DE}^{tot}(\text{CH}_y) = 34.6 [1 + 0.29y] \left(1 - \frac{E_{th}}{E} \right)^{3.0} \frac{1}{E} \ln(e + 0.15E) (\times 10^{-16} cm^2) \quad (16)$$

where E_{th} and E are the threshold and collision energy, respectively, expressed in eV, and $e = 2.71828\dots$ is the basis of natural logarithm. It is seen that σ_{DE}^{tot} has

proper physical behavior both in the threshold region and at high energies (Born-Bethe asymptotics). (The value of E_{th} in the total cross section is that of the dissociative channel of CH_y with smallest energy threshold.) Eq.(16) also reflects the linear increase of σ_{DE}^{tot} with the increase of the number of hydrogen atoms in CH_y . The partial cross section for a particular neutral dissociation channel A of CH_y is given by

$$\sigma_{DE}(A/CH_y) = R_{DE}(A/CH_y) \cdot \sigma_{DE}^{tot}(CH_y) \quad (17)$$

where the value of branching ration $R_{DE}(A/CH_y)$ is given in Table 2 for each dissociation channel. The values of threshold energies, E_{th} , for individual dissociative channels are also given in that table.

3.3 Dissociative Excitation of CH_y^+ by Electron Impact

Similarly as in the case of CH_y dissociation to neutrals, the total cross sections for dissociative excitation of CH_y^+ ($y = 1-4$) ions by electron impact, determined in sub-section 2.3., can all be represented by the analytic expression

$$\sigma_{DE}^{tot}(CH_y^+) = 29.4 [1 + 0.71(y - 1)] \left(1 - \frac{E_{th}}{E}\right)^{2.5} \frac{1}{E} \ln(e+0.9E) (\times 10^{-16} cm^2) \quad (18)$$

where E_{th} and E are the threshold and collision energy, expressed in eV, and $e = 2.71828\dots$

The partial cross sections of the individual dissociative excitation channels are given by

$$\sigma_{DE}(A^+/CH_y^+) = R_{DE}^+(A^+/CH_y^+) \cdot \sigma_{DE}^{tot}(CH_y^+) \quad (19)$$

where $R_{DE}^+(A^+/CH_y^+)$ is the branching ratio of the channel A^+ from the dissociation of CH_y^+ ion. The values of R_{DE}^+ and E_{th} for each dissociative excitation channel of CH_y^+ ions are given in Table 3.

For the capture-auto-ionisation dissociation cross section of CH^+ ions discussed at the end of sub-section 2.3, we have the following analytic expression

$$\sigma_{CAD}^{tot}(C^+/CH^+) = 20.6 \left(1 - \frac{2.5}{E}\right)^{2.5} \frac{1}{E} \ln(e + 0.9E) (\times 10^{-16} cm^2) \quad (20)$$

where we took into account that the threshold for this reaction is $E_{th} \simeq 2.5$ eV.

3.4 Dissociative Ionisation of CH_y^+ by electron impact

The cross section data determined as described in sub-section 2.4 for the total dissociative ionisation of CH_y^+ ions can be fitted to the following analytic expression:

$$\sigma_{DI}^{tot}(CH_y^+) = 31.0 [1 + 0.086(y - 1)] \left(1 - \frac{E_{th}}{E}\right)^{1.55} \frac{1}{E} \ln(e+0.5E) \quad (\times 10^{-16} cm^2) \quad (21)$$

where E and E_K are in eV units, and the values for E_{th} are given in Table 4. It should be remarked that the y-dependence of $\sigma_{DI}^{tot}(CH_y^+)$ is relatively weak.

With the above expression for $\sigma_{DI}^{tot}(CH_y^+)$ and the values of branching ratios $R_{DI}^+(A^+/CH_y^+)$ from Table 4 one can calculate the partial DI cross sections $\sigma_{DI}(A^+/CH_y^+)$ for any particular $CH_y^+ \rightarrow A^+ + H^+ + e$ reaction channel (see Eq.(14)).

3.5 Dissociative Recombination of Electrons with CH_y^+

For break-up reactions (such as the electron dissociative recombination with molecular ions), Wigner predicted [68] that the reaction cross section should behave as E^{-1} , as long as there are no other competing processes. The experimental data on $e + CH_y^+$ dissociative recombination (DR) all confirm this general behavior for sufficiently low collision energies. At higher collision energies (above $\sim 1 - 2$ eV), resonance structures appear in the total recombination cross section, indicating that indirect mechanisms begin to contribute to the recombination, and that the dissociating state (or states) may be strongly coupled with other reaction channels (e.g. auto-ionisation of doubly excited dissociating state, processes involving the high Rydberg states of the molecule, etc.). As we have seen earlier, the thresholds of competing dissociative excitation channels of CH_y^+ , appear at 5 - 10 eV, and at these and higher collision energies the DR cross section should start to fall off more rapidly than E^{-1} with increasing E . Combining these facts, and averaging over the resonance structures, the total cross section σ_{DR}^{tot} for dissociative recombination of CH_y^+ ions can be represented in the form

$$\sigma_{DR}^{tot}(CH_y^+) = \frac{A}{E^\alpha \cdot (1 + aE)^\gamma} \quad (\times 10^{-16} cm^2) \quad (22)$$

where E is the collision energy (in eV) and A , α , a and γ are some constants. In accordance with the Wigner law, the value of α should be close to one. However, Eq.(22) is only an analytic fit function and the values of parameters A , α , a and γ

are determined from the experimental data given in a wide energy range ($10^{-3} - 20$ eV) by criteria of fit optimization. With the analytic function given by Eq.(22) we have fitted the experimental data for CH_y^+ from storage-ring experiments [44, 51, 52] (averaging over the resonance structures), and only for CH_4^+ we have used for the fit the old (corrected) merged-beams data [49]. The obtained values for the fitting parameters in Eq.(22) are given in Table 8. The fits cover the energy range $10^{-4} - 20$ eV (for CH_4^+ the upper limit is ~ 5 eV), but their extension to higher energies should be considered as reasonable.

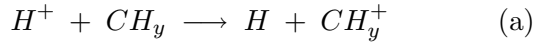
The cross sections for the individual recombination channels are obtained by multiplying the total cross section with the corresponding branching ratio,

$$\sigma_{DR}(A/\text{CH}_y^+) = R_{DR}(A/\text{CH}_y^+) \cdot \sigma_{DR}^{tot}(\text{CH}_y^+) \quad (23)$$

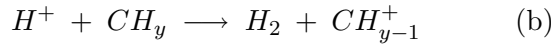
where the values of branching ratios R_{DR} are given in Table 5. It can be assumed (in the spirit of Wigner's law) that the values of these ratios will remain the same as long as the resonances do not dominate the cross section behavior.

3.6 Charge Exchange and Particle Exchange Processes

The cross sections for pure charge exchange (electron capture)



and particle exchange (or rearrangement)



processes in the thermal energy region (≤ 0.05 eV) can be related to their thermal rate coefficients, $R_{CX}^{(a),(b)} \cdot K_{CX}^{tot}$, by the relations

$$\sigma_{CX}^{(a)} = 7.26 \cdot \frac{R_{CX}^{(a)} \cdot K_{CX}^{tot}}{E^{1/2}} \quad (\times 10^{-16} \text{cm}^2) \quad (24\text{a})$$

$$\sigma_{CX}^{(b)} = 7.26 \cdot \frac{R_{CX}^{(b)} \cdot K_{CX}^{tot}}{E^{1/2} + cE^\gamma} \quad (\times 10^{-16} \text{cm}^2) \quad (24\text{b})$$

where K_{CX}^{tot} (in units of $10^{-9} \text{cm}^3/\text{s}$) and branching ratios $R_{CX}^{(a),(b)}$ are given in Table 6, $c = 0.8$, $\gamma = 2.5$, and E is the collision energy, in eV. The values of constants c and γ have been chosen to ensure that for energies above ≈ 1 eV, the particle exchange channel constitutes not more than $\sim 10\%$ of $\sigma_{CX}^{(a)}$. The expressions (24) for $\sigma_{CX}^{(a)}$ and $\sigma_{CX}^{(b)}$ are not expected to be valid for energies above ~ 0.1 eV. However, Eq.(24a) can serve as a good low-energy limit of the cross section for the pure electron capture process (a).

The charge exchange cross section in $H^+ + C_xH_y$ collisions have been fitted in Ref.[8] by using a polynomial fit based on the Chebishev polynomials. In the present report we use an analytic expression for σ_{CX} which provides physically correct behavior of the cross section outside of the range of fitted data as well. The analytic form for $\sigma_{CX}^{(a)}$ is

$$\sigma_{CX}^{(a)} = \frac{a_1}{E^{1/2} + a_2 E^{a_3}} + \frac{b_1 \exp(-b_2/E^{b_3})}{E^{b_4} + b_5 E^{b_6} + b_7 E^{b_8} + b_9 E^{b_{10}}} (\times 10^{-16} cm^2) \quad (25)$$

where a_i and b_i are fitting parameters and the collision energy E is expressed in eV units. The values of fitting parameters are given in Table 9. The above analytic representation of $\sigma_{CX}^{(a)}$ is valid from thermal to MeV energies.

The cross section for reaction $H^+ + C \rightarrow H + C^+$ can be taken from Ref.[69]. Its analytic fit has the form [69]

$$\sigma_{CX}(E) = c_1 \left[\frac{\exp(-c_2/E)}{1 + c_3 E^2 + c_4 E^{4.5}} + c_5 \frac{\exp(-c_6 E)}{E^{c_7}} \right] (\times 10^{-16} cm^2) \quad (26)$$

where the energy E is expressed in units of KeV and the fitting parameters are: $c_1 = 14.2$, $c_2 = 0.686$, $c_3 = 1.96 \cdot 10^{-3}$, $c_4 = 1.49 \cdot 10^{-9}$, $c_5 = 18.9$, $c_6 = 10.2$ and $c_7 = -3.02$.

4 Reaction Rate Coefficients

The cross section of an electron impact reaction with CH_y and CH_y^+ , averaged over a Maxwellian velocity distribution of electrons, gives the rate coefficient for that reaction (we use the units $m_e = 1$, $k_B = 1$, k_B being the Boltzmann constant)

$$\langle \sigma v \rangle = \frac{4}{\pi^{1/2} u^3} \int_{v_{th}}^{\infty} v^3 \sigma(v) e^{-\frac{v^2}{u^2}} \cdot dv \quad (27)$$

where $u = (2T)^{1/2}$, T is the electron temperature, v is the electron collision velocity, and v_{th} is the velocity corresponding to the reaction threshold energy ($v_{th} = (2E_{th})^{1/2}$).

For the charge exchange reactions, we assume that the protons have a Maxwellian velocity distribution characterized by a temperature $T = m_p u^2/2$, and that the hydrocarbons have certain kinetic energy $\varepsilon = MV^2/2$. The charge exchange reaction rate coefficient is then defined as

$$\langle \sigma v \rangle = \frac{1}{\pi^{1/2} u V} \int_0^{\infty} v_r^2 \sigma(v_r) \left(e^{-\frac{(v_r - V)^2}{u^2}} - e^{-\frac{(v_r + V)^2}{u^2}} \right) \cdot dv_r \quad (28)$$

where $v_r = |\vec{u} - \vec{V}|$ is the relative collision velocity, and we have taken into account that the considered charge exchange reactions are all exothermic. In Eq.(28), thus, ε appears as parameter.

With the analytic expressions for the cross sections provided in the preceding section, the computation of corresponding reaction rate coefficients is straightforward. Some of these analytic expressions also allow to calculate $\langle \sigma v \rangle$ in closed analytic form.

With the expression (15) for electron impact ionisation cross section, the corresponding rate coefficient, in units (cm^3/s), has the form (using Ref.[70])

$$\langle \sigma v \rangle_{ion} = 8.76 \cdot 10^{-5} \frac{1}{I_c} \left(\frac{\beta}{2\pi I_c} \right)^{1/2} \cdot \left[A_0 E_1(\beta) + \sum_{j=1}^N A_j \cdot j! \cdot e^{-\beta/2} \cdot \mathcal{W}_{-j;1/2}(\beta) \right] \quad (29)$$

where $\beta = I_c/T$, $E_1(-\beta) = -E_i(-\beta)$ is the exponential integral, $\mathcal{W}_{-j;1/2}(\beta)$ is the Whittaker function, and I_c and T are expressed in eV units.

The total cross section expressions for dissociative excitation of CH_y to neutrals, Eq.(16), and dissociative excitation and ionisation of CH_y^+ , Eqs.(18) and (21), respectively, can also be integrated over the Maxwellian distribution of electron velocity in closed form. The analytical result in this case, however, is only approximate. By writing the total cross section for these processes in the form

$$\sigma = A_0(y) \left(1 - \frac{E_{th}}{E} \right)^\alpha \frac{1}{E} \ln(e + cE) \quad (30)$$

the rate coefficient takes the form

$$\langle \sigma v \rangle = \frac{8A_0(y)E_{th}}{\pi^{1/2}u^3} \int_1^\infty \left(1 - \frac{1}{x} \right)^\alpha \ln(e + ax) e^{-\beta x} dx \quad (31)$$

where $a = cE_{th}$ and $\beta = E_{th}/T$. With the values of parameter c and E_{th} for the processes involved, the product $a = cE_{th}$ is always larger than one, and for $ax \geq 1$ the function $\ln(e + ax)$ can be represented (with an accuracy better than 1%) by the expression

$$\ln(e + ax) \simeq \frac{2.62}{1 + ax} + \ln(ax). \quad (32)$$

Then Eq.(31) reduces to

$$\langle \sigma v \rangle = \frac{8A_0(y)E_{th}}{\pi^{1/2}u^3} (\mathcal{I}_1 + \mathcal{I}_2 + \mathcal{I}_3) \quad (33)$$

where

$$\mathcal{I}_1 = 2.62 \int_1^\infty \frac{1}{1+ax} \left(1 - \frac{1}{x}\right)^\alpha e^{-\beta x} dx, \quad (34a)$$

$$\mathcal{I}_2 = \ln(a) \int_1^\infty \left(1 - \frac{1}{x}\right)^\alpha e^{-\beta x} dx, \quad (34b)$$

$$\mathcal{I}_3 = \int_1^\infty \left(1 - \frac{1}{x}\right)^\alpha \ln(x) e^{-\beta x} dx. \quad (34c)$$

The integral \mathcal{I}_2 is given in Ref.[70] and has the form

$$\mathcal{I}_2 = \ln(a) \left(\frac{1}{\beta} \Gamma(1 + \alpha) e^{-\beta/2} \mathcal{W}_{-\alpha; 1/2}(\beta) \right), \quad (35)$$

where $\Gamma(x)$ is the gamma function. Keeping in mind that the main contribution to the integral \mathcal{I}_1 comes from the region $x \simeq 1$, the factor $(1+ax)^{-1}$ can be replaced by $(1+a)^{-1}$. Then the integral is reduced to the form of \mathcal{I}_2 and has the solution

$$\mathcal{I}_1 = \frac{2.62}{1+a} \left(\frac{1}{\beta} \Gamma(1 + \alpha) e^{-\beta/2} \mathcal{W}_{-\alpha; 1/2}(\beta) \right). \quad (36)$$

The main contribution to the integral (34c) comes from the region of larger x . Hence, retaining the first term only in the expansion of $(1 - 1/x)^\alpha$ in powers of $1/x$, one obtains approximately

$$\mathcal{I}_3 \simeq \frac{1}{\beta} E_1 \beta \equiv -\frac{1}{\beta} E_1(-\beta), \quad (37)$$

where $E_1(\beta)$ is the exponential integral function. (The neglected terms are related to the higher order Schlömilch's exponential integrals, $E_n(\beta)$.)

In order to obtain the rate coefficient in cm^3/s units, the expression (33), in which σ was expressed in units of cm^2 , should be multiplied by the atomic unit of velocity, $v_0 = 2.19 \times 10^8 \text{ cm/s}$. (E_{th} and T , as before, are expressed in eV units.)

With the expression (22) for the total cross section for dissociative recombination of electrons with CH_y^+ ions, the integration in Eq.(28) for $\langle \sigma v \rangle$ can also be carried out analytically and the result is [70]:

$$\langle \sigma v \rangle_{DR}^{tot} = \frac{8A}{\pi^{1/2} (2T)^{3/2}} \frac{1}{a^{2-\alpha}} \beta_1^{\gamma+\alpha-3} e^{\beta_1/2} \Gamma(2-\alpha) \mathcal{W}_{\frac{\alpha-1-\gamma}{2}; \frac{2-\alpha-\gamma}{2}}(\beta_1) \quad (38)$$

where A , a , α , γ are the parameters in Eq.(22), and $\beta_1 = 1/aT$. In order to obtain $\langle \sigma v \rangle_{DR}^{tot}$ in units of cm^3/s , Eq.(38) should be multiplied by the atomic unit of velocity, $v_0 = 2.19 \cdot 10^8 \text{ cm/s}$, with T being expressed in eV.

The Whittaker function $\mathcal{W}_{\lambda,\mu}(z)$ and the exponential integral $E_1(z)$, in terms of which the rate coefficient for electron impact processes are expressed, have the following asymptotic behaviour for high values of their argument [70]

$$\mathcal{W}_{\lambda,\mu}(z) \approx z^\lambda e^{-z/2} \left[1 + \frac{\mu^2 - (\lambda - 1/2)^2}{z} + \mathcal{O}(1/z^2) \right] \quad (39)$$

$$E_1(z) \approx \frac{1}{z} e^{-z} \left[1 - \frac{1}{z} + \frac{2}{z^2} + \mathcal{O}(1/z^3) \right] \quad (40)$$

With these expansions one can easily obtain the leading terms of rate coefficients of electron-impact processes at low temperatures.

The averaging of charge exchange cross sections Eqs.(24a) and (24b) (valid in the thermal energy region) over the Maxwellian velocity distribution can easily be performed by assuming that the kinetic energy ε of hydrocarbon molecules is zero. Then, as is well known, the rate coefficient for the electron capture process, described by Eq.(24a), is constant, while for the particle exchange channel (Eq. (24b)) it tends to a constant value when T tends to the thermal values (below ~ 0.05 eV). For temperatures of interest in the context of magnetic fusion edge plasmas (temperatures above 0.5 eV) and for hydrocarbon molecules with non-zero kinetic energy (as they come from the walls or are produced in dissociation processes), the calculation of charge exchange rate coefficients should be performed by using Eq. (31) with the expression (25) for σ_{cx} . This integration cannot be carried out in a way so as to obtain a result in compact analytical form.

5 Concluding Remarks

In this report we have presented a collisional database for the most important electron and proton impact processes with the hydrocarbon molecules CH_y ($y = 1 - 4$) and their ions CH_y^+ . These processes are given by Eqs. (1) - (6). Although the cross sections for these processes are given in a wide collision energy range (from the threshold to several KeV for electron-impact excitation and ionisation processes, and from thermal to several hundred KeV/AMU for proton impact charge exchange), the selection of the processes for inclusion in the present report was done on the basis of their expected important role in fusion edge plasmas with temperatures up to about 50 eV. On this basis, processes such as further ionisation of CH_y^+ by electron impact, or dissociative charge exchange, which have sufficiently high thresholds (above $\approx 30 - 40$ eV), and, therefore, small cross sections at energies below $\approx 50 - 60$ eV, have been excluded from the scope of the present

report. The cross section database for these processes and collision systems is also virtually non-existent.

The present database is aimed mainly for hydrocarbon transport studies in fusion edge plasmas and, therefore, the question of quantum states of reaction products (which may be important in the context of plasma spectroscopy studies) has not been addressed.

In establishing the present database all the cross section information presently available for the considered processes has been taken into account. Since this information is by far incomplete, well established semi-empirical cross section scaling relationships have been used to derive the cross sections which were unavailable in the literature. This approach, nevertheless, introduces uncertainties in the derived cross sections, particularly in the near threshold region, where the scaling relations become less reliable. The confidence in the determination of the cross sections in this region (below $\approx 20 - 30$ eV) originates from the fast increase of the cross sections in this region according to the power law $(1 - E_{th}/E)^\alpha$ with $\alpha \approx 2 - 3$ (observed for the experimentally available cross sections).

A particular attention was given in the present report to account accurately for the different channels in dissociative excitation, ionisation, and recombination processes. Experimental cross section information exists for the majority of dissociative channels. The branching ratios of the dissociative recombination channels are experimentally known for all CH_y^+ ions (except for CH_4^+ , where it has been determined by interpolation). For the dissociative excitation of CH_y to neutrals and CH_y^+ , the channel cross sections were determined using arguments based on the application of additivity rules for the strength of chemical bonds and the similarity (or identity) of dissociation mechanisms with those of the dissociative ionisation.

All cross sections for the reaction channel considered are expressed by analytical functions of relatively simple form. Tables of the fitting parameters are provided. Except for the case of charge exchange, for all other considered processes the reaction rate coefficients are also calculated in analytic form, expressed, however, in terms of Whittaker- and exponential-integral functions.

The graphs of the cross sections and rate coefficient for all studied reactions as well as the analytic fitting coefficients are provided for downloading on the web-domain www.eirene.de of the EIRENE code, in the atomic and molecular data section.

An additional effort has been made to determine the energetics (average energy lost by the projectile and gained by the products) for each reaction. This in-

formation, required in the kinetic transport modeling codes, or for plasma cooling studies, is given in Tables 1 – 6.

The accuracy of provided cross sections varies for the various processes considered. For electron impact ionisation reactions it is about 10 – 15% for the cross sections based on experimental information, and 15 – 30% for those derived by using the semi-empirical scalings. For dissociative excitation of CH_y (to neutrals) and CH_y^+ by electron impact the uncertainties of derived cross sections are larger and may reach 50 – 100%. In certain cases, however, such as the neutral dissociation of CH_4 and the H^+ and H_2^+ ion production channels of dissociative excitation, this uncertainty is much smaller, about 20 – 30% or less. Similar accuracies have also the cross sections for dissociative ionisation of CH_y^+ ions.

The cross sections for electron - CH_y^+ dissociative recombination are believed to be accurate to within 20 – 30%, although the total recombination cross section, based on recent storage-ring data, should be much more accurate (10 – 15%). The charge exchange cross section for CH_4 , based on the available experimental data is believed to be accurate to within 15 – 20% in the entire energy range. For the other CH_y hydrocarbon molecules the derived cross sections have much larger uncertainties: 30 – 50% for energies below ~ 1 eV and above ~ 1 KeV/AMU and even more for the energies in between; for CH_3 these uncertainties should be somewhat smaller.

Because the energies of excited dissociating states of CH_y and CH_y^+ systems are unavailable in the literature (except for CH and CH^+), the estimated average electron energy loss and total kinetic energy of products in dissociative electron impact reactions have uncertainties of about 1 - 2 eV. For the weak processes (usually having a large energy threshold) this uncertainty may be even higher. These processes, however, play only a minor role in the reaction kinetics.

6 References

References

- [1] “Technical Basis for the ITER Final Design Report”; ITER EDA Documentation Series No.16 (IAEA, Vienna, Austria, 1998).
- [2] P.C.Stangeby “Some observations about the current state of edge plasma physics”, presented at IAEA TCM on divertor concepts, Aix-en-Provence, France, Sept. 2001, submitted to Plasma Physics and Controlled Fusion.
- [3] W.E. Hofer and J. Roth, eds., “Physical Processes of Interaction of Fusion Plasmas with Solids”; (Academic Press, San Diego, 1996).
- [4] A.A. Haasz, J.A. Stephens, E. Vietzke et al., Atom. Plasma-Mater. Interac. Data Fusion, Vol. 7 (part A) (1998), p. 5.
- [5] A.B. Ehrhardt and W.D. Langer, “Collisional Processes of Hydrocarbons in Hydrogen Plasmas”, Report PPPL-2477 (1987), (Princeton Plasma Physics Laboratory, Princeton USA).
- [6] D.A. Alman, D.N. Ruzic and J.N. Brooks, Phys. Plasmas 7, 1421 (2000).
- [7] R.K. Janev, J.G. Wang, I. Murakami and T. Kato, “Cross Sections and Rate Coefficients for Electron-Impact Ionisation of Hydrocarbon Molecules”, Res. Report NIFS-DATA-68 (2001) (National Institute for Fusion Science, Toki, Japan).
- [8] R.K. Janev, J.G. Wang and T. Kato, “Cross Sections and Rate Coefficients for Charge Exchange Reactions of Protons with Hydrocarbon Molecules”, Res. Report NIFS-DATA-64 (2001) (National Institute for Fusion Science, Toki, Japan).
- [9] D. Reiter, “The EIRENE Code”, see <http://www.eirene.de>
- [10] D. Rapp and P. Englander-Golden, J. Chem. Phys. 43, 1464 (1965).
- [11] B.L. Schram, M.J. van der Wiel, F.J. de Heer, and H.R. Moustafa, J. Chem. Phys. 44, 49 (1966).
- [12] N. Duric, I. Cadez and M.V. Kurepa, Int. J. Mass Spectrom. Ion Processes 108, R1 (1991).

- [13] W. Hwang, Y.-K. Kim and M.E. Rudd, *J. Chem. Phys.* 104, 2956 (1996).
- [14] Y.-K. Kim, M.A. Ali and M.E. Rudd, *J. Res. NIST* 102, 693 (1997).
- [15] H.C. Straub, D. Lin, B.G. Lindsey et al, *J. Chem. Phys.* 106, 4430 (1997)
- [16] C. Tian and C.R. Vidal, *J. Phys. B: At. Mol. Opt. Phys.* 31, 895 (1998).
- [17] B. Adamczyk, A.J.H. Boerboom, B.L. Schram and J. Kistemaker, *J. Chem. Phys.* 44, 4460 (1966).
- [18] H. Chatham, D. Hills, R. Robertson and A. Gallagher, *J. Chem. Phys.* 81, 1770 (1984).
- [19] O.J. Orient and S.K. Srivastava, *J. Phys. B: At. Mol. Opt. Phys.* 20, 3923 (1987).
- [20] F.A. Baiocchi, R.C. Wetzel and R.S. Freund, *Phys. Rev. Lett.* 53, 771 (1984).
- [21] V. Tarnovsky, A. Levin, H. Deutsch and K. Becker, *J. Phys. B: At. Mol. Opt. Phys.* 29, 139 (1996).
- [22] H.M. Rosenstock, K. Draxl, B.M. Steiner and J.T. Herron, *J. Phys. Chem. Ref. Data* 6 (suppl. 1) (1977).
- [23] S.W. Benson and J.H. Buss, *J. Chem. Phys.* 29, 546 (1958).
- [24] D.R. Bates, *Int. J. Mass Spectrom. Ion Processes* 8, 1 (1987).
- [25] C.E. Melton, *J. Chem Phys.* 37, 562 (1962).
- [26] H.D.P. Liu and G. Verhaegen, *J. Chem. Phys.* 53, 735 (1970).
- [27] S. Green, P.S. Bagus, B. Liu et al., *Phys. Rev. A* 5, 1614 (1972).
- [28] E.F. van Dishoeck, *J. Chem. Phys.* 86, 196 (1987).
- [29] H. Takagi, N. Kosugi and M. Le Dourneuf, *J. Phys. B:* 24, 711 (1991).
- [30] G.D. Flesh, R.E. Utecht and H.J. Svec, *Int. J. Mass Spectrom. Ion Processes*, 58, 151 (1984).
- [31] T. Ogawa, H. Tomura, K. Nakashima and H. Kawazumi, *Chem. Phys.* 113, 65 (1987).

-
- [32] T. Ogawa, J. Kurawaki and M. Higo, Chem. Phys. 61, 181 (1981).
- [33] T.G. Finn, B.L. Carnahan, W.C. Wells and E.C. Zipf, J. Chem. Phys. 63, 1596 (1975).
- [34] J.A. Schiavone, D.E. Donohue and R.S. Freund, J. Chem. Phys. 67, 759 (1977).
- [35] R. Locht, J.L. Olivier and J. Momigny, Chem. Phys. 43, 425 (1979).
- [36] R. Locht and J. Momigny, Chem. Phys. 49, 173 (1980).
- [37] T. Nakano, H. Toyoda and H. Sugai, Jpn. J. Appl. Phys. 30, 2912 (1991).
- [38] T. Nakano and H. Sugai, Jpn. J. Appl. Phys. 31, 2919 (1992).
- [39] H.F. Winters, J. Chem. Phys. 63, 3462 (1975).
- [40] H.F. Winters, and M. Inokuti, Phys. Rev. A 25, 1420 (1982).
- [41] R.L. Platzman, Radiation Res. 17, 419 (1962).
- [42] D.A. Vroom and F.J. de Heer, J. Chem. Phys. 50, 573 (1969).
- [43] P. Forck, PhD thesis, Ruprecht-Karls-Universität, Heidelberg, (1994) (unpublished, cross section quoted in Ref.[45]).
- [44] Å. Larson, A. Le Padellec, J. Semaniak et al., Ap. J. 505, 459 (1998).
- [45] N. Djuric, Y.S. Chung, B. Wallbang, and G.H. Dunn, Phys. Rev. A 56, 2887 (1997).
- [46] N. Djuric, S. Zhou, G.H. Dunn and M.E. Bannister, Phys. Rev. A 58, 304 (1998).
- [47] Z.Amitay D. Zajfman, P. Forck, et al., Proc. 14th Conf. on the Applications of Accelerators in Research and Industry, Denton 1996, AIP Conf. Proc. 392, 51 (1997)
- [48] Y.-K. Kim, K.K. Irikura and M.A. Ali, J. Res. NIST 105, 285 (2000).
- [49] P.M. Mul, J.B.A. Mitchell, V.S. D'Angelo et al. J. Phys. B. 14, 1353 (1981).
- [50] J.B.A. Mitchell, Phys. Rep. 186, 215 (1990).

-
- [51] Z. Amitay, D. Zajfman, P. Forck et al., *Phys. Rev. A* 54, 4032 (1996).
- [52] L. Vejby-Christensen, L.H. Andersen, O. Heber et al., *Ap. J.* 483, 531 (1997).
- [53] J. Semaniak, Å. Larson, A. Le Padellec et al., *Ap. J.* 498, 886 (1998).
- [54] D.R. Bates, *Ap. J.* 306, L45 (1986).
- [55] S. Green and E. Herbst, *Ap. J.* 229, 121 (1979).
- [56] S. Datz et al., *Phys. Rev. Lett.* 74, 896 (1995).
- [57] D.J. Koopman, *J. Chem. Phys.* 49, 5203 (1968).
- [58] J.G. Collins and P. Keberle, *J. Chem. Phys.* 46, 1082 (1967).
- [59] L.H. Toburen, Y. Nakai and R.A. Langley, *Phys. Rev.* 171, 114 (1968).
- [60] M. Elliot, *J. de Physique* 38, 24 (1977).
- [61] S.L. Varghese, G. Bissinger, J.M. Joyce and R. Laubert, *Nucl. Instrum. Methods*, 170, 269 (1980)
- [62] M.L. Jones, B.L. Dougherty, T. Dillingham et al., *Nucl. Instrum. Methods, B:* 10/11, 142 (1985).
- [63] T. Kusakabe, K. Asahina, A. Iida et al., *Phys. Rev. A* 62, 062715 (2000).
- [64] T. Kusakabe, R. Buenker and M. Kimura, *At. Plasma-Mater. Interac. Data Fusion*, 10, xxx (2002)
- [65] B.M. Smirnov, "Asymptotic Methods in the Theory of Atomic Collisions", (Nauka, Moscow, 1973) (in Russian).
- [66] T.J. Millar, P.R.A. Facquhar and K. Willacy, *Astron. Astrophys. Suppl.* 121, 139 (1997).
- [67] K.L. Bell, H.B. Gilbody, J.G. Hughs et al., *J. Phys. Chem. Ref. Data* 12, 891 (1983)
- [68] E.P. Wigner, *Phys. Rev.* 73, 1002 (1948).
- [69] P.C. Stancil, J.-P. Gu, C.C. Havener et al., *J. Phys. B* 31, 3647 (1998).
- [70] I.S. Gradshteyn and I.M. Ryzhik, "Tables of Integrals, Series and Products", (Academic Press, New York, 1965).

7 Appendix: Tables

Table 1

Ionisation (I_p) and Appearance (A_p) Potentials for CH_y ($1 \leq y \leq 4$)
 Dissociative Ionisation Channels (Ref.[22]) and Reaction Energetics
 ($\overline{E}_k = \kappa D_0, \kappa = 0.3$ normally).

Reaction	I_p or A_p (eV)	$\overline{E}_{el}^{(-)}$ (eV)	\overline{E}_K (diss. Products) (eV)
$e + CH_4 \rightarrow CH_4^+ + 2e$ (*)	12.63	12.63	—
$\rightarrow CH_3^+ + H + 2e$ (*)	14.25	14.55	0.3 ($\kappa=0.8$)
$\rightarrow CH_2^+ + H_2 + 2e$ (*)	15.1	17.10	2.0 ($\kappa=0.8$)
$\rightarrow CH^+ + H_2 + H + 2e$ (*)	19.9	22.05	2.15
$\rightarrow C^+ + 2H_2 + 2e$	19.6	21.64	2.04
$\rightarrow H^+ + CH_3 + 2e$	18.0	19.91	1.91
$\rightarrow H_2^+ + CH_2 + 2e$	20.1	22.36	2.26
$e + CH_3 \rightarrow CH_3^+ + 2e$ (*)	9.84	9.84	—
$\rightarrow CH_2^+ + H + 2e$ (*)	15.12	16.74	1.62
$\rightarrow CH^+ + H_2 + 2e$	15.74	17.41	1.67
$\rightarrow C^+ + H_2 + H + 2e$	19.50	22.42	2.92
$\rightarrow H^+ + CH_2 + 2e$	18.42	21.00	2.58
$\rightarrow H_2^+ + CH + 2e$	20.18	23.28	3.1
$e + CH_2 \rightarrow CH_2^+ + 2e$ (*)	10.40	10.40	—
$\rightarrow CH^+ + H + 2e$ (*)	15.53	16.93	1.40
$\rightarrow C^+ + H_2 + 2e$	14.67	15.97	1.30
$\rightarrow H^+ + CH + 2e$	18.01	20.30	2.29
$\rightarrow H_2^+ + C + 2e$	18.83	21.37	2.54
$e + CH \rightarrow CH^+ + 2e$ (*)	10.64	10.64	—
$\rightarrow C^+ + H + 2e$ (*)	14.74	15.99	1.25
$\rightarrow H^+ + C + 2e$ (*)	17.07	19.02	1.95

(*): Reaction channels included in the database of Ref.[5] .

Note: $\overline{E}_{el}^{(-)} = A_p + \overline{E}_K$

Table 2Neutral Dissociation Channels of CH_y ,Threshold Energies, E_{th} , Mean Electron Energy Loss, $\overline{E}_{el}^{(-)}$,and Mean Total Energy of the Products, \overline{E}_K .

Reaction Channel	R_{DE}	$E_{th}=\overline{E}_{el}^{(-)}$ (eV)	\overline{E}_K (products) (eV)
$e + CH_4 \rightarrow CH_3 + H + e$ (*)	0.760	6.6	2.2 ($\kappa=0.5$)
$\rightarrow CH_2 + H_2 + e$	0.144	7.0	2.3 ($\kappa=0.5$)
$\rightarrow CH + H_2 + H + e$	0.073	12.0	3.0
$\rightarrow C + 2H_2 + e$	0.023	10.6	2.5
$e + CH_3 \rightarrow CH_2 + H + e$ (*)	0.83	6.9	2.3 ($\kappa=0.5$)
$\rightarrow CH + H_2 + e$	0.14	7.2	2.36 ($\kappa=0.5$)
$\rightarrow CH + 2H + e$	0.02	12.4	3.1
$\rightarrow C + H_2 + H + e$	0.03	10.6	2.5
$e + CH_2 \rightarrow CH + H + e$ (*)	0.90	6.4	2.1 ($\kappa=0.5$)
$\rightarrow C + H_2 + e$	0.08	6.6	3.3 ($\kappa=1$)
$\rightarrow C + 2H + e$	0.02	10.4	2.6
$e + CH \rightarrow C + H + e$ (*)	1.0	5.3	1.8

(*): Reaction channels included in the database of Ref.[5].

Notes:

1) $\overline{E}_K = \kappa D_0$, $\kappa = 0.3$ normally.2) $E_{th} = D_0 + \overline{E}_K$

Table 3Dissociative Excitation Channels of CH_y^+ ,Threshold Energies, E_{th} , Mean Electron Energy Loss, $\overline{E}_{el}^{(-)}$,and Mean Total Kinetic Energy of the Products, \overline{E}_K .

Reaction Channel	R_{DE}^+	$E_{th}=\overline{E}_{el}^{(-)}$ (eV)	\overline{E}_K (products) (eV)
$e + CH_4^+ \rightarrow CH_3^+ + H + e$ (*)	0.360	3.5	1.3 ($\kappa=0.8$)
$\rightarrow CH_3 + H^+ + e$ (*)	0.315	8.29 (#)	1.91
$\rightarrow CH_2^+ + H_2 + e$	0.140	4.5	2.01 ($\kappa=0.8$)
$\rightarrow CH_2 + H_2^+ + e$	0.073	9.77 (#)	2.25
$\rightarrow CH^+ + H_2 + H + e$	0.068	9.33	2.15
$\rightarrow C^+ + 2H_2 + e$	0.044	8.85	2.04
$e + CH_3^+ \rightarrow CH_2^+ + H + e$ (*)	0.256	7.03	1.62
$\rightarrow CH_2 + H^+ + e$ (*)	0.515	11.18 (#)	2.58
$\rightarrow CH^+ + H_2 + e$	0.125	7.22	1.67
$\rightarrow CH + H_2^+ + e$	0.048	11.3 (#)	3.1
$\rightarrow C^+ + H_2 + H + e$	0.056	12.65	2.92
$e + CH_2^+ \rightarrow CH^+ + H + e$ (*)	0.195	6.08	1.4
$\rightarrow CH + H^+ + e$ (*)	0.675	9.0 (#)	2.29
$\rightarrow C + H + H^+ + e$	0.040	14.53	3.35
$\rightarrow C^+ + H_2 + e$	0.056	5.62	1.3
$\rightarrow C + H_2^+ + e$	0.021	11.6 (#)	2.54
$\rightarrow C^+ + 2H + e$	0.013	11.52	2.66
$e + CH^+ \rightarrow C^+ + H + e$ (*)	0.09	6.5 (§)	2.5 (§)
$\rightarrow C + H^+ + e$ (*)	0.91	5.0 (#)	1.5 (§)

(*): Channels included in Ref.[5]

(#): Experimental threshold energies, Refs.[45,46]

(§): Obtained from Ref.: A.J. Lorquet et al., J.Chem.Phys. **55**, 4053 (1971)

Table 4

Main reaction channels in dissociative ionisation of CH_y^+ :

branching ratios, R_{DI}^+ , threshold energies, E_{th} ,

mean electron energy loss, $\overline{E}_{el}^{(-)}$ ($= E_{th}$),

and mean total kinetic energy of ionic products, $\overline{E}_K(\text{ion.prod.})$

($\overline{E}_K(\text{neutr.prod.}) = 0$)

Reaction	Channel	R_{DI}^+	$E_{th} = \overline{E}_{el}^{(-)}$ (eV)	\overline{E}_K (ion.prod.) (eV)
$e + \text{CH}_4^+$	$\rightarrow e + \text{CH}_3^+ + \text{H}^+ + e$	0.33	27.05	11.78
	$\rightarrow e + \text{CH}_2^+ + \text{H} + \text{H}^+ + e$	0.24	32.48	11.78
	$\rightarrow e + \text{CH}^+ + \text{H}_2 + \text{H}^+ + e$	0.23	33.09	11.78
	$\rightarrow e + \text{C}^+ + \text{H}_2 + \text{H} + \text{H}^+ + e$	0.20	36.76	11.78
$e + \text{CH}_3^+$	$\rightarrow e + \text{CH}_2^+ + \text{H}^+ + e$	0.39	30.81	11.78
	$\rightarrow e + \text{CH}^+ + \text{H} + \text{H}^+ + e$	0.30	35.94	11.78
	$\rightarrow e + \text{C}^+ + \text{H}_2 + \text{H}^+ + e$	0.31	35.09	11.78
$e + \text{CH}_2^+$	$\rightarrow e + \text{CH}^+ + \text{H}^+ + e$	0.55	30.41	11.78
	$\rightarrow e + \text{C}^+ + \text{H} + \text{H}^+ + e$	0.45	34.15	11.78
$e + \text{CH}^+$	$\rightarrow e + \text{C}^+ + \text{H}^+ + e$	1.00	29.0	11.78

Table 5

Dissociation Channels in $e + CH_y^+$ Recombination,
their Branching Ratios, R_{DR} , and Total Kinetic Energy

$E_K^{(0)}$ of the Products (in their ground states and for $E_{el} = 0$).

Reaction Channel	R_{DR}	$E_K^{(0)}$ (eV)	Excited products for $E \leq 1eV$
$e + CH_4^+ \rightarrow CH_3 + H$ (*)	0.21	8.17	$CH_3(3s); CH_3(3p)$
$\rightarrow CH_2 + H_2$	0.09	7.83	$CH_2(a; b; c; d)$
$\rightarrow CH_2 + H + H$ (*)	0.43	3.30	$CH_2(a; b)$
$\rightarrow CH + H_2 + H$	0.25	3.42	$CH(a; A; B)$
$\rightarrow C + H_2 + H_2$	0.02	4.43	$C(^1D; ^1S)$
$e + CH_3^+ \rightarrow CH_2 + H$ (*)	0.40	4.97	$CH_2(a; b; c)$
$\rightarrow CH + H_2$	0.14	5.10	$CH(a; A; B; C)$
$\rightarrow CH + H + H$	0.16	0.64	$CH(a; A)$
$\rightarrow C + H_2 + H$	0.30	1.57	$C(^1D)$
$e + CH_2^+ \rightarrow CH + H$ (*)	0.25	6.00	$CH(a; A; B; C)$
$\rightarrow C + H_2$	0.12	7.00	$C(^1D; ^1S)$
$\rightarrow C + H + H$	0.63	2.47	$C(^1D; ^1S)$
$e + CH^+ \rightarrow C + H$ (*)	1.00	7.18	$C(^1D; ^1S)$
$e + CH^+ \rightarrow C(^1D) + H(1S)$	0.75 (#)	5.92	
$\rightarrow C(^1S) + H(1S)$	0.25 (#)	4.50	
for $E_{el}(CM) \leq 0.9$ eV			
$e + CH^+ \rightarrow C(^1D) + H(1S)$	0.075 (#)	5.92	
$\rightarrow C(^1S) + H(1S)$	0.025 (#)	4.50	
$\rightarrow C(^3P^0) + H(1S)$	0.25 (#)	-0.30	
$\rightarrow C(^1P^0) + H(1S)$	0.20 (#)	-0.50	
$\rightarrow C(^3D^0) + H(1S)$	0.45 (#)	-0.76	
for $E_{el}(CM) = 0.9 - 9$ eV			

(*): Channels included in Ref.[5].

(#): From Ref.[51].

Table 6

Charge Exchange Reaction in $H^+ + CH_y$ Thermal Collisions;
 Total Thermal Rate Coefficients, K_{CX}^{tot} , Branching Ratios, R_{CX} ,
 and Reaction Exothermicities, ΔE .

Reaction Channel	$K_{CX}^{tot} (10^{-9} cm^3/s)$	R_{CX}	ΔE (eV)
$H^+ + CH_4 \rightarrow H + CH_4^+ (*)$	3.8	0.4	1.1 (#)
$\rightarrow H_2 + CH_3^+$	3.8	0.6	2.96
$H^+ + CH_3 \rightarrow H + CH_3^+ (*)$	3.4	1.0	3.78 (#)
$H^+ + CH_2 \rightarrow H + CH_2^+ (*)$	2.8	0.36	3.2
$\rightarrow H_2 + CH^+$	2.8	0.64	5.17
$H^+ + CH \rightarrow H + CH^+ (*)$	1.9	0.31	2.47
$\rightarrow H_2 + C^+$	1.9	0.69	5.28
$H^+ + C \rightarrow H + C^+ (*)$	—	—	2.33

(*): Reaction channels included in the database of Ref.[5]

(#): These exothermicities are absorbed by reaction products

Table 7

Values for the fitting coefficients in Eq.(15) for the total and partial ionisation cross sections in $e + CH_y$ collisions. For each process I_c and A_i (i from 1 to N) are listed. 5.1090E+02 means 5.1090×10^2 .

e + C

Cross section

process	I_c	$A_i, i=1-3$		
$e + C \rightarrow$ ionisation	1.1260E+01	2.1143E+00	-1.9647E+00	-0.6084E+00

e + CH

(a) Total cross section

process	I_c	$A_i, i=1-3$ $A_i, i=4-6$ $A_i, i=7-8$		
$e + CH \rightarrow$ total ionisation	1.1200E+01	1.2258E+00 -1.4891E+02 5.1090E+02	-3.0764E+00 4.3224E+02 -1.5314E+02	2.6182E+01 -6.6387E+02

(b) Partial cross sections

process	I_c	$A_i, i=1-3$ $A_i, i=4-6$		
$e + CH \rightarrow CH^+ + 2e$	1.1300E+01	1.4439E+00 9.2822E+00	-1.2724E+00 -1.5506E+01	-2.2221E+00 8.2778E+00
$e + CH \rightarrow C^+ + H + 2e$	1.4800E+01	4.3045E-01 3.2957E+00	-4.1305E-01 -5.6549E+00	-5.6881E-01 3.4295E+00
$e + CH \rightarrow C + H^+ + 2e$	1.7140E+01	4.4144E-02 2.3115E+00	-1.8579E-02 -4.1040E+00	-4.1046E-01 2.7436E+00

$e + \text{CH}_2$

(a) Total ionisation

process	I_c	$A_i, i=1-3$			$A_i, i=4-6$		
$e + \text{CH}_2 \rightarrow \text{total ionisation}$	1.0910E+01	2.9597E+00	-2.6451E+00	-3.7136E+00	8.9168E+00	-1.2872E+01	5.8594E+00

(b) Partial cross sections

process	I_c	$A_i, i=1-3$			$A_i, i=4-6$		
$e + \text{CH}_2 \rightarrow \text{CH}_2^+ + 2e$	1.0400E+01	1.7159E+00	-1.7164E+00	-6.5529E-01	2.1724E+00	-5.4186E+00	3.1616E+00
$e + \text{CH}_2 \rightarrow \text{CH}^+ + \text{H} + 2e$	1.5530E+01	8.1919E-01	-7.5016E-01	-3.8063E-03	1.4065E+00	-3.6447E+00	2.6220E+00
$e + \text{CH}_2 \rightarrow \text{C}^+ + \text{H}_2 + 2e$	1.7100E+01	3.8400E-02	-2.91786E-02	-0.98490E-01	0.73008E+00	-1.2111E+00	0.85722E+00
$e + \text{CH}_2 \rightarrow \text{CH} + \text{H}^+ + 2e$	2.2300E+01	-5.8168E-02	8.2064E-02	5.2048E-02	3.1915E-01	-1.3363E-01	2.3477E-01
$e + \text{CH}_2 \rightarrow \text{C} + \text{H}_2^+ + 2e$	2.4800E+01	2.7682E-02	5.0215E-02	3.7494E-04	5.1300E-01	-6.1525E-01	6.2835E-01

$e + \text{CH}_4$

(a) Total cross section

process	I_c	$A_i, i=1-3$			$A_i, i=4-6$		
$e + \text{CH}_4 \rightarrow \text{total ionisation}$	1.2630E+01	2.3449E+00	-2.6163E+00	2.1843E-01	1.0890E+01	-2.9718E+01	2.4582E+01

(b) Partial cross sections

process	I_c	$A_i, i=1-3$			$A_i, i=4-6$		
$e + \text{CH}_4 \rightarrow \text{CH}_4^+ + 2e$	1.2630E+01	1.3541E+00	-1.4665E+00	1.6787E-01	6.1801E+00	-1.5638E+01	1.0767E+01
$e + \text{CH}_4 \rightarrow \text{CH}_3^+ + \text{H} + 2e$	1.4010E+01	1.6074E+00	-1.4713E+00	-2.7386E-01	1.9556E-01	1.1343E-01	9.0166E-03
$e + \text{CH}_4 \rightarrow \text{CH}_2^+ + \text{H}_2 + 2e$	1.6200E+01	1.6252E-01	-1.0708E-01	-3.2252E-01	8.7125E-01	-1.8747E-02	1.3071E-01
$e + \text{CH}_4 \rightarrow \text{CH}^+ + \text{H}_2 + \text{H} + 2e$	2.2200E+01	-1.2458E-01	1.6287E-01	-3.3395E-01	3.5738E+00	-5.0472E+00	2.8240E+00
$e + \text{CH}_4 \rightarrow \text{C}^+ + 2\text{H}_2 + 2e$	2.2000E+01	-6.2138E-02	4.4747E-02	1.7054E-01	-2.2989E-01	7.7426E-01	-2.9020E-01
$e + \text{CH}_4 \rightarrow \text{CH}_2 + \text{H}_2^+ + 2e$	2.2300E+01	-1.7615E-02	1.8347E-02	-5.0664E-02	2.6118E-01	1.5316E-01	-1.7314E-01
$e + \text{CH}_4 \rightarrow \text{CH}_3 + \text{H}^+ + 2e$	2.1100E+01	-3.4698E-01	-1.6026E-02	4.3296E+00	-1.5155E+01	2.4766E+01	-1.0873E+01

Table 8Values of Fitting Parameters in Eq.(22) for the $e + CH_y^+$ Systems.

Collision System	A	a	α	γ
$e + CH_4^+$	3.0	0.1	1.25	1
$e + CH_3^+$	4.8	0.8	1.10	0.5
$e + CH_2^+$	6.7	1.2	1.15	0.5
$e + CH^+$	3.16	0.13	0.75	1.0

Table 9

Values of Fitting Parameters in Eq.(25)

Parameter	CH	CH_2	CH_3	CH_4
a_1	4.28	7.32	17.0	3.93
a_2	0.001	0.005	385.0	445.0
a_3	3.0	3.0	2.5	2.3
b_1	20.2	20.95	51.3	46.2
b_2	5.3	1.55	0.00	0.00
b_3	0.35	0.57	—	—
b_4	0.00	0.00	0.096	0.094
b_5	$1.12 \cdot 10^{-6}$	$2.35 \cdot 10^{-7}$	$2.0 \cdot 10^{-9}$	$9.0 \cdot 10^{-6}$
b_6	1.45	1.55	2.00	1.2
b_7	$1.10 \cdot 10^{-20}$	$5.86 \cdot 10^{-21}$	$5.5 \cdot 10^{-21}$	$2.845 \cdot 10^{-18}$
b_8	4.3	4.26	4.3	3.8
b_9	0.00	0.00	0.00	$5.81 \cdot 10^{-22}$
b_{10}	—	—	—	4.4